A Critical Review on the Vulnerability Assessment of Natural Gas Pipelines Subjected to Seismic Wave Propagation. Part 2: Pipe Analysis Aspects

Grigorios Tsinidis[1], Luigi Di Sarno[2], Anastasios Sextos[3], and Peter Furtner[4]

[1]University of Sannio, Italy & Vienna Consulting Engineers ZT GmbH, Austria
[2]University of Sannio, Italy & University of Liverpool, United Kingdom
[3]University of Bristol, United Kingdom & Aristotle University of Thessaloniki, Greece
[4]Vienna Consulting Engineers ZT GmbH, Austria

Corresponding Author: Dr Grigorios Tsinidis, Vienna Consulting Engineers ZT GmbH, Austria, Untere Viaduktgasse 2, 1030, Vienna, email: tsinidis.grigorios@gmail.com

Abstract: The socio-economic and environmental impact, in case of severe damage on Natural Gas (NG) pipeline networks, highlights the importance of a rational assessment of the structural integrity of this infrastructure against seismic hazards. Up to date, this assessment is mainly performed by implementing empirical fragility relations, while a limited number of analytical fragility curves have also been proposed recently. The critical review of available fragility relations for the assessment of buried pipelines under seismically-induced transient ground deformations, presented in the first part of this paper, highlighted the need for further investigation of the seismic vulnerability of NG pipeline networks, by employing analytical methodologies, capable of simulating effectively distinct damage modes of this infrastructure. In this part of the paper, alternative methods for the analytical evaluation of the seismic vulnerability of buried steel NG pipelines are presented. The discussion focuses on methods that may appropriately simulate buckling failures of buried steel NG pipelines since these constitute critical damage modes for the structural integrity of this infrastructure, when subjected to seismically-induced transient ground deformations. Salient parameters that control the seismic response and vulnerability of buried pressurized steel pipelines and therefore should be considered by the relevant analytical methods, such as the operational pressure of the pipeline, the geometric imperfections of the pipeline walls, the trench backfill properties, the site characteristics and the spatial variability of the seismic ground motion along the pipeline axis, are thoroughly discussed. Finally, a new approach for the assessment of buried steel NG pipelines against seismically-induced buckling failures is introduced. Through the discussion, recent advancements in the field are highlighted, whilst acknowledged gaps are identified, providing recommendations for future research.

Keywords: Natural gas pipelines; fragility; soil-pipe interaction; transient ground deformations; steel pipelines; buckling

1. Introduction

Earthquake-induced damages on Natural Gas (NG) and fossil-fuel pipeline networks may lead to significant downtimes, which in turn may result in high direct and indirect economic losses, not only for the affected area and state, but also internationally. Moreover, severe damages may trigger ignition or explosions with life-treating consequences and significant effects on the environment. The above aspects highlight the importance of simple, yet efficient, seismic analysis and vulnerability assessment methods to be used for the design of new NG networks, as well as the evaluation of the vulnerability and resilience of existing networks. Up to date, the seismic vulnerability assessment of this infrastructure is mainly performed by implementing empirical fragility relations. A limited number of analytical fragility curves that compute probabilities of failure in the 'classical sense' have also been proposed recently (Lee et al., 2016; Jahangiri and Shakid, 2018). A critical review of available fragility relations for buried pipelines, subjected to seismically-induced transient ground deformations, was presented in the first part of this paper (Tsinidis et al. 2019). Through the detailed discussion, a general lack of analytical fragility relations for a rigorous seismic vulnerability assessment of buried steel NG pipelines was highlighted. This was partly attributed to the absence of optimum seismic Intensity Measures *IMs* for this infrastructure, which may correlate effectively with diverse seismically-induced damage modes. The above knowledge shortfalls highlight the need for efficient analytical methodologies, which may allow for a thorough investigation of the vulnerability of steel buried NG pipelines against distinct seismically-induced damage modes. In this context, a thorough overview of alternative analytical methodologies for the vulnerability assessment of buried steel NG pipelines under seismically-induced transient ground deformations, is presented in this part of the paper. The discussion focuses on the buckling failures, which constitute critical damage modes for the structural integrity of steel buried pipelines subjected to transient ground deformations. Salient parameters that control the seismic response and vulnerability of buried steel NG pipelines and therefore should be considered by the relevant analytical methods are thoroughly discussed. Finally, a new approach for the vulnerability assessment of steel buried NG pipelines against seismically-induced buckling failures is introduced. Through the discussion, recent advancements in the field are highlighted, whilst acknowledged gaps are identified.

2 Analytical methods to define the EDP-IM relationship

A critical step in the quantitative seismic vulnerability assessment of any element at risk, e.g. a buried steel NG pipeline, is the development of structure-specific analytical fragility curves that provide a functional relationship between the *EDP* and the selected seismic *IM* on the basis of predictions of relevant numerical analyses (Jalayer et al., 2017; Bakalis & Vamvatsikos, 2018). Various approaches have been proposed in the literature for this purpose, including the incremental dynamic analysis (IDA), the multiple-stripe analysis and the cloud

analysis. In the framework of an IDA, a series of dynamic analyses are conducted, by employing an adequate nonlinear model of the investigated structural system and using a suite of accelerograms, which are progressively scaled upwards in amplitude, so as to cover a wide range of seismic *IM* levels. Through these analyses the evolution of *EDP* with increasing seismic intensity level is reported, in the so-called IDA curves (Vamvatsikos and Cornell, 2002). A similar approach is followed in multiple-stripe analysis. However, in this type of analysis the selected ground shaking motions do not necessarily scaled to reach various intensity levels. Instead use of different sets of scaled or unscaled records at each *IM* level is made, in an effort to reflect the site-specific seismic hazard at each *IM* level (Jalayer and Cornell, 2009). In cloud analysis un-scaled or scaled ground seismic motions are used. Typically, only a single record will correspond to each seismic IM level, while scaled records may be used to capture higher order damage states (Bakalis and Vamvatsikos, 2018; Miano et al., 2018). This approach will result for a cloud of points in the *EPD-IM* plot. A probabilistic relation between the *EDP* and the *IM* is then established on the basis of a regression analysis (Jalayer et al., 2015).

Regardless of the selected method, a critical step in the fragility assessment of a structure is the development of an adequate numerical methodology that will account for the majority of salient parameters that control the seismic response of the structure, being at the same time computationally efficient. Both Lee et al. (2016) and Jahangiri and Shakib (2018) performed IDA analyses to examine numerically the seismic vulnerability of buried steel NG pipelines and propose analytical fragility relations. However both studies disregarded critical parameters that affect the seismic response and vulnerability of buried steel NG pipelines.

3 Parameters affecting the response of buried steel pipelines under transient ground deformations

3.1 Soil-pipe interaction effects

The response of embedded civil infrastructure subjected to seismic wave propagation is manifested by the transient ground displacements induced by the surrounding ground, while the inertia-related effects are of minor -if not negligible- importance (Hashash et al., 2001). This observation, which is valid even for large embedded structures, such as tunnels, has been reflected to various design codes and guidelines for embedded infrastructures (EN 1998-4, 2006) and may further imply that the inertial soil-structure interaction effects are minor and insignificant. Based on this remark, various pseudo-static analysis methods have been developed for embedded structures, such as tunnels and pipelines (ALA, 2001; FHWA 2009; ISO 23469 2005). Actually, several recent studies have compared the predictions of simplified pseudo-static analyses methods and approaches for tunnels against full dynamic analyses results, as well as experimental data from dynamic centrifuge tests, revealing reasonably good comparisons (e.g. Tsinidis et al., 2015; Lanzano et al., 2015; Tsinidis et al., 2016). Since the

mass of buried pipelines is much lower than that of extended embedded structures, the effect of inertial SSI effects is expected to be even less important for buried pipelines.

Depending on the type of the dominant seismic wave (*S*-waves, *P*-waves or surface waves) and the alignment of the pipeline axis to the ray path, pipelines may be subjected to either pure axial compression or tension, bending in the horizontal or vertical plane, or a combination of the above. The differential movement between the pipe and the surrounding ground, the distinct response of the spatially variable soil deposits that a pipeline may cross, as well as the spatially variable ground seismic motion along the pipeline axis, are among the parameters that may induce a non-uniform shear stress field along the soil-pipe interface, which in turn may lead to non-uniform axial stresses on the pipeline. The latter may impose axial buckling or tensile rupture failures on the pipeline. Flexural stresses may be caused on an embedded pipe by a direct introduction of soil curvature on it. These stresses can cause flexural failures, such as bending buckling or excessive ovalization of the pipe section. Generally, the axial strains that are induced on straight embedded pipelines due to transient ground deformations are larger than the bending ones and actually dominate the response (Hindy and Novak, 1979). Bending strains are generally higher than axial strains near pipe bends (Karamanos, 2016).

3.2 Geologic / geotechnical conditions of the site and distance to the seismic source

Not surprisingly, the geologic, geomorphic and geotechnical conditions of the site of interest, affect significantly the transient ground deformations that are being induced on a buried pipeline and therefore its seismic response and vulnerability. Regardless of the selected method of analysis, a reliable knowledge of the degree of soil stiffness variation along the pipeline axis, as well as of the soil stiffness gradient with depth, or the potential inclination of the bedrock and other topographic characteristics, such as basins, hill crests and toes and embankments, are parameters that may affect considerably the transient ground deformations along the pipeline axis.

If the soil site of interest is relatively uniform, strains on extended pipelines can arise only by the apparent propagation velocity of the seismic waves, or by large relative soil-pipe motion, when the seismic shaking amplitude is large. Even under these circumstances, the expected strain levels on the pipe are commonly smaller than the yield strain of the steel grades that are used in NG pipeline applications. In the presence of strong soil heterogeneities or special topographic characteristics along the pipeline axis, increased ground deformations and subsequent straining of the pipeline are expected, due to effects of the above site characteristics on the wavefield. Generally, these site conditions may alter significantly the frequency content of the ground seismic motion, leading to an amplification of the ground displacement grandients.

The level of knowledge of the soil site characteristics determines the selection of the adequate analysis or assessment method for a buried pipeline. Evidently, for uniform soil sites the use of complex and sophisticated numerical models and tools is not required. For complex sites, soil

response analyses, preferably in 2D or 3D, in combination with the use of soil-pipe interaction models that can capture the axial response of the pipe and the relevant potential failures (e.g. shell buckling) are recommended. Field surveys may contribute in gathering information related to the site characteristics. Obviously, the above procedure is applicable in the design of new pipeline networks, as well as for the pre-seismic assessment of existing networks, since it is associated with a high computational effort and requires significant time to be performed.

As highlighted in the first part of this paper, the proximity of the site of interest to the seismic source determines the dominating seismic waves on the site, as well as their frequency content. A pipeline located near the seismic source is expected to be stricken by vertically propagated body waves (e.g. *S*-waves) of high amplitude and frequency content. On the other hand, a buried pipeline in a site away from the earthquake source is expected to be stricken by a combination of nearly-vertically propagated body waves and surface waves (e.g. *R*-waves). The predominant wavelength of the surface waves is expected to control the axial straining of the pipeline (O' Rourke M.J. and Hmadi, 1988). Summarizing, the distance of the site of interest to the seismic source is expected to affect the characteristics of the seismic ground motion and therefore should be considered in the relevant analysis or assessment framework. The identification of the expected dominant seismic waves for the seismic vulnerability assessment of an extended NG pipeline network could be informed by the results of a preliminary seismic hazard analysis, the latter carried out for carefully selected seismic scenarios.

3.3 Internal pressure

Steel pipelines used in transmission NG networks are commonly pressurized to high levels, reaching pressures as high as 8-9 MPa. For this uniform pressure level, steel pipelines develop large initial circumferential tensile stresses, which interact with axial straining caused by potential seismically-induced transient ground deformations, leading to a rather complicated axial response. The restriction of buried pipelines by the surrounding trench soil alters the combined effects of the above loading conditions, further complicating the axial response. The combined effects of internal pressurization and axial compression of free and restrained cylindrical steel shells has been investigated before, both numerical and experimentally (Timoshenko and Gere, 1961; Yun and Kyriakidis, 1990; Paquette and Kyriakides, 2006; Kyriakides and Corona, 2007). To further elaborate on the axial response of steel NG pipelines, a series of compression static analyses were performed by the authors on above ground and embedded segments of API 5L X65 steel pipelines. Various parameters that affect the axial response of steel pipelines, namely the diameter over thickness (D/t) ratio of the pipe segment, the internal pressure level, the existence of imperfections on the walls of the pipe segment (further discussed in the following section) and the characteristics of the trench soil surrounding the buried pipe segments, were considered. The analyses were performed by employing the finite element code ABAQUS (ABAQUS, 2012). Figure 1 illustrates

representative numerical models of pipe segments developed in the context of this short study. The pipeline segments were simulated with inelastic shell elements, while the trench soil, surrounding the embedded segments, was simulated by means of linear elastic solid elements. The pipe-soil interface was simulated by means of an advanced hard contact interaction model, available in ABAQUS (2012). The shear response of the soil-pipe interface was obeying a classical Coulomb friction model, described by a friction coefficient μ = 0.3. The segments were subjected to a pure axial stress that was introduced in terms of axial deformation on the one end-side of the segment, with the other end-side being constrained. More details about the simulation may be found in Tsinidis et al. (2018).

During axial compressive loading the examined segments are subjected to plastic buckling, which results in a drop of their axial stiffness and a significant increase of axial deformations. Contrary to elastic shell buckling, where the collapse is sudden, in plastic buckling the failure is separated from the first instability (Kyriakides and Corona, 2007). This response was also verified herein.

Figure 2 compares average axial load-deformation paths computed for above ground and equivalent embedded pipe segments. The results, which refer to segments of steel pipelines with diameters 406.4 mm (16 in) and 1219.2 mm (48 in) and radius over thickness ratios *R/t* = 19.7 and 25.6, respectively, are presented in normalized forms. In particular, the axial loading is normalized by the yield axial load of the section: $P_o = 2\pi Rt\sigma_y$ (Paquette and Kyriakides, 2006), where the yield stress σ_y = 448 MPa. The normalized axial load is plotted against the average axial shortening δ_x/l, where δ_x is the axial deformation of the segment and l is the initial length of the segment. The trench soil in case of embedded pipes is characterized by a density ρ = 1.8 t/m^3, a shear modulus G = 23.4 MPa, and a Poisson's ratio, ν = 0.33. The consideration of internal pressure results in a general lowering of the axial load-displacement path. In parallel, the internal pressure leads the limit loading to occur at progressively higher axial shortening levels δ_x/l. This response, which has been verified experimentally by Paquette and Kyriakides (2006), is attributed to the plastic interaction of the two loading conditions, i.e. internal pressure and axial compression, acting on the segment. Generally, the confinement, which is offered by the trench soil, 'stabilizes' the axial response of embedded segments, leading to an increase of the axial load-deformation response compared to the one of the equivalent above ground segments, i.e. higher critical loadings and 'critical' shortening levels are identified for embedded segments compared to the ones of the equivalent above ground segments. Finally, the critical stresses and the 'critical' axial shortening levels are both decreasing with increasing *R/t* ratio. The main observation is that the internal pressure level can affect considerably the seismic response and vulnerability of NG steel pipelines and therefore, this parameter should be considered by the selected analysis method.

3.4 Geometric imperfections of steel pipelines

The axial compression response of thin-walled steel cylindrical shells is known to be highly affected by geometric imperfections. Actually, these imperfections may reduce significantly the actual buckling critical loading of a steel cylindrical shell, compared to the one predicted by theoretical elastic solutions (NASA, 1968). Operations related to manufacturing process, girth welding, transportation and laying may lead to deviations of the pipeline walls from perfect geometry. These imperfections, which are referred as geometric imperfections, are commonly considered in numerical analyses by linearly superposing eigenmode shapes, the latter obtained by an eigenvalue buckling analysis of the examined pipe shell. An alternative approach is to simulate the imperfection by means of a geometric stress-free perturbation in the initial geometry and mesh of the examined shell (e.g. Yun and Kyriakidis, 1990; Psyrras at al., 2019). Variations of pressure on the pipeline walls caused by the surrounding trench soil along the axis of the pipeline may also results in a kind of 'load' imperfections.

Yun and Kyriakidis (1990) reported that the presence of even low-magnitude axisymmetric geometric imperfections may reduce significantly the bifurcation and limit stress and strain of a steel pipeline, compared to those predicted for a 'perfect' geometry. This observation was verified by the results of the short numerical parametric study, discussed in the previous section. In particular, the study considered both 'perfect' segments and segments with geometry perturbation. For the latter cases, a stress-free, biased axisymmetric imperfection was assumed at a short zone of 1.0 m, which was set at the middle of the segment. The imperfection was defined following Paquette and Kyriakides (2006) and Psyrras et al. (2019), having a maximum amplitude of 10 % of the pipe wall thickness (i.e. w/t = 0.1). The imperfection level was based on relevant specifications from NG pipeline manufactures. ArcelorMittal for example specifies a manufacturing tolerance for the walls of API-5L X65 pipelines in the range of + 15% to -12.5% (ArcelorMittal 2018). As seen in Figure 2, the critical loadings of imperfect segments, as well as the axial shortening levels, where these loadings are observed (i.e. 'critical' axial shortening levels), are both lower compared to those predicted for the equivalent 'perfect'/ segments. The differences on the computed paths of perfect and equivalent imperfect segments are generally higher for non-pressurized segments, while they decrease significantly with the increase of internal pressure. Actually, for pressurized pipe segments with the maximum allowable operational pressure (i.e. $p = 0.72 \times p_y$) the differences on the loading-deformation paths of equivalent perfect and imperfect segments are negligible for $\delta_x / l < 0.5 - 0.8$ (depending on the R/t ratio of the examined segment). Additionally, the differences between the axial response of perfect and imperfect buried segments are smaller compared to those revealed for above ground segments, particularly for higher levels of internal pressure.

The amplitude of initial geometric imperfection may also be a critical parameter for the axial response of steel pipelines. Figure 3a compares average axial force-deformation paths computed for above ground segments of a steel pipeline with diameter D = 406.4 mm and

radius over thickness ratios R/t = 19.7, considering various levels of geometric imperfection amplitudes. The comparisons are plotted for both non-pressurized and pressurized segments. The axial response of the segments reduces with increasing imperfection amplitude (i.e. lower responses are reported for w/t = 0.2). This is generally more evident in case of non-pressurized segments (i.e. for p = 0). The pressurization of the segments reduces the detrimental effect of initial geometric imperfections. Similar conclusions are drawn for the equivalent buried segments (Figure 3b). The confinement that is offered by the trench soil reduces the effect of imperfection on the axial response of the examined segments, particularly for the cases of pressurized segments. Actually, for the pressurized segment with the maximum allowable operational pressure level ($p = 0.72 \times p_{max}$), the axial force-deformation paths predicted by the analyses of equivalent perfect and imperfect segments are quite similar, if not identical, even in the post-buckling regime.

Evidently, the geometric imperfections of the walls of a steel pipe are affecting significantly its response under axial compressive straining and therefore they should be considered by the selected design of vulnerability assessment method. The only way to simulate accurately these imperfections is by means of shell elements with a quite refined mesh. The available analytical studies on the seismic vulnerability assessment of NG pipelines (Lee et al., 2016; Jahangiri and Shakib, 2018) have modelled the examined pipelines by means of inelastic beam elements and fibers, disregarding the critical effect of geometric imperfections.

3.5 Trench soil

The properties of the trench soil, surrounding a buried pipeline, are another critical parameter that might affect the seismic response and vulnerability of a steel pipeline. After the installation of the pipeline, the excavated trench is backfilled, with the backfill material being compacted. The compaction might increase the lateral earth pressure coefficient to values higher than unity, which subsequently may lead to an increasing frictional resistance of the soil-pipe interface. This increasing shear resistance of the soil-pipe interface may lead to higher axial stresses and strains on the pipeline under seismically-induced transient ground deformations. In this context, a critical issue for the rigorous assessment of buried steel pipelines is the simulation of the shear response of the soil-pipe interface. The shear response of the soil-pipe interface is commonly simulated through the classical Coulomb model, which correlates the shear stresses developed along the soil-pipe interface with the soil normal pressures acting on the pipe, through the friction coefficient μ. Generally, the friction coefficient of the soil-pipe interface varies along the axis of a long pipeline while it may fluctuate during ground seismic shaking. However, for steel pipelines without external coating it is bounded to the following limits, $\mu_{min} = 0.3$ and $\mu_{max} = 0.8$. These limits are actually derived from the linear relation between the friction coefficient μ and friction angle φ of the trench soil, i.e. $\mu = (0.5 - 0.9) \times \tan\varphi$, which was proposed by O'Rourke and Hmadi (1988) and is commonly

adopted in practice. For typical sand backfills the soil friction angle can range between 29° and 41-44°, yielding to above limits for the friction coefficients. It is worth noticing that friction coefficient of the soil-pipe interface may be affected by the level of scour of the external face of the steel pipeline since the scour reduces the frictional resistance along the soil-pipe interface. Additionally, the existence of external pipe coating might lead to different friction coefficients for the soil-pipe interface. ALA (2001) suggests the interface angle δ to be estimated as follows: $\delta = f\,\varphi$, where φ the internal friction of the soil and f a coating parameter depending on the coating material (e.g. 0.6, 0.9 and 1.0 for Polyethylene, Coal Tar and Concrete, respectively). The friction coefficient μ may then be computed as $\mu = \tan\delta$.

The dimensions and stiffness of the trench soil are other parameters that might also affect the seismic response of a buried pipeline. The commonly used assumption of an infinitely large trench may lead to an underestimation of the actual response of a pipeline subjected to lateral ground seismic motion, as highlighted by Kouretzis et al. (2013) and Chaloulos et al. (2015, 2017).

Figure 4 elaborates on the effect of trench soil stiffness on axial compression response of embedded steel pipelines. In particular, the axial force-deformation paths computed for a steel pipeline with diameter D = 1066.8 mm (40 in) and ratio over thickness ratio R/t = 27.9, embedded in trench soils with different stiffnesses, are compared. The comparisons are provided for both non-pressurized and pressurized segments, with either considering or neglecting the initial geometric imperfections of the segments walls. Solid lines correspond to the results referring to the trench soil with reduced stiffness, while dashed lines stand for the analyses, where higher soil stiffness was considered for the trench. The increase of the stiffness of the trench soil, results in an increased stabilization of the pipe segments, which in turn, results in an increase of their axial response. This observation is more evident for the non-pressurized pipe segments.

The trench soil compliance is commonly simulated in a simplified way via discrete soil springs and dashpots. Despite the computational efficiency of such a simulation approach, potential geometric nonlinearities along the soil-pipe interface response can not be thoroughly accounted for, particularly when the effect of geometric imperfections on the pipe walls are considered as a perturbation of the pipeline geometry and mesh. The proper selection of the stiffness and damping coefficients for soil springs and dashpots elements, respectively, is another critical issue that remains still not full addressed (see *Section 4.2*). The alternative simulation of the trench soil by means of 3D solid elements in a coupled simulation of an 'infinitely' long soil-pipe configuration is computationally inefficient, particularly in the framework of a large number of numerical analyses that are required for the seismic vulnerability assessment of buried pipelines. Some other alternatives are discussed in the ensuing (*Section 4.3*).

3.6 Spatial variation of the ground seismic motion along the pipeline axis

Ground seismic motion is varying in space and time in terms of wave amplitude, phase, frequency characteristics and duration. Given the complicated nature of the mechanisms that cause this phenomenon and the numerous parameters and uncertainties involved, the so-called spatial variability of seismic ground motion can only be investigated stochastically. The factors that contribute to the spatial variability of seismic ground motion can be grouped into three main effects, i.e. the *wave passage effect*, the *ray-path effect* and the *local site effect* (Figure 5). The wave passage effect is associated with the finite velocity, with which the seismic waves are traveling. This phenomenon results in different arrival times of the seismic waves to various locations of the site. The ray-path effect is the result of the continuous reduction of coherency of seismic waves due to successive reflections and refractions that take place along their propagation through heterogeneous soil sites or due to the superposition of wave emanating from different points of the seismic source. The latter effect is also known as *extended source effect*. Finally, the local soil conditions may affect significantly characteristics of the ground seismic motion, such as the amplitude, frequency content and duration.

Evidently, the spatial variation of the ground seismic motion along the axis of an extended structure, such as a NG pipeline, is expected to affect significantly its response. Indeed, the spatial variation of the ground seismic motion across the length of extended structures, such as bridges, was found to affect considerably their response (e.g. Sextos et al., 2003; Sextos and Kappos, 2009; Zerva, 2009). A common approach to account for these phenomena is to implement deterministic time history analyses, introducing spatially variable ground motions, while random vibration analysis is another alternative. The effect of incoherent ground seismic motion on the seismic response of pipelines has been investigated by Zerva et al. (1985) and Zerva (1994). Using random vibration analysis on analytical models of continuous and segmented pipelines, the researchers reported a higher level of stresses on the pipelines under partially correlated motions, compared to those predicted for perfectly coherent motions. Similar observations may be found in more recent studies (e.g. Lee et al., 2009).

Soil inhomogeneities, special subsurface geomorphic conditions or irregular topography (e.g. hills, canyons, valleys etc) may cause local site effects, which may amplify significantly the ground seismic motion (e.g. Scandella and Paolucci, 2010; Gelagoti et al., 2010; Riga et al., 2018), resulting in high ground deformations on the pipelines. The critical effect of inhomogeneous soil sites on the pipeline seismic response has been reported by numerical, analytical and experimental studies (e.g. Hindy and Novak, 1979; Nishio et al. 1983; Liang 1995). Recently, Psyrras and Sextos (2018) proposed some idealized cases of soil sites, which might be crucial for the seismic response of a crossing pipeline, i.e. a site consisting of two horizontally adjacent soil layers with highly distinct properties and a site with a soft alluvial valley of trapezoid shape, laying within a stiff soil or soft rock. The researchers highlighted that for these site conditions, an amplification of the transient ground deformations is expected near the soil boundaries (i.e. at the vertical interface of the two soil layers or at the valley

edges) under vertically propagated seismic *S*-waves, which may lead to significant axial or bending strains on a buried steel pipeline crossing these sites, depending on the position of the pipeline axis compared with the polarization of the seismic waves. In a more recent study, Psyrras et al. (2019) examined the potential of buckling of buried steel NG pipelines, crossing the above idealized soil sites, under seismically-induced transient ground deformations, highlighting that under particular circumstances, an appreciable axial stress concentration may be observed near the soil discontinuities, which may even lead to buckling failures.

3.7 Elbows and other restrictions

Elbows are pipe bends, which under ground seismic shaking reveal a more complex behaviour compared to the straight parts of the pipeline and may generally affect the response of buried pipelines. Various numerical and experimental studies have focused on the response of these elements under seismic and static loading conditions, the latter associated to seismically-induced permanent ground deformations, such as faulting (e.g. Shinozoka and Koike, 1979; Saberi et al., 2013; Hamada et al., 2000; Yoshizaki et al., 2003; Karamitros et al., 2016; Karamanos, 2016, among others).

Connections of the pipelines with stiffer structures, e.g. metering or pressure reduction stations, may impose restrictions on the pipelines during ground seismic shaking, leading to significant increases of axial or bending stresses locally. The effects of these restrictions on the seismic vulnerability of steel NG pipelines have not been thoroughly studied.

3.8 Summary

A series of parameters that may affect the response and therefore the vulnerability of buried steel NG pipelines were reported in this section. The consideration of the above parameters in relevant vulnerability studies depends on the capabilities of the numerical method that is employed each time.

4 Analysis methods for the seismic vulnerability assessment of buried steel NG pipelines

Various methodologies may be found in the literature for the seismic analysis and vulnerability assessment of buried pipelines, which can generally be classified as methods that neglect the soil-pipe interaction (SPI) phenomena and methods that account for the SPI phenomena in either a simplified or more detailed manner. A brief overview of the available methods is presented in ensuing, focusing on the applicability and efficiency of each method in the framework of a seismic vulnerability assessment study. A more detailed review of available methods may be found elsewhere (e.g. Datta et al. 2001; Psyrras and Sextos, 2018).

4.1 Analysis methods neglecting the soil-pipe interaction phenomena – 'free-field' methods

The main assumption of these analysis methods is that the embedded structure, the buried pipeline herein, is forced to conform perfectly to the movement of the surrounding ground; in other words, the pipe strains are identical to the ones of the surrounding ground. These approaches commonly adopted in the practice for buried structures, whose stiffness is much smaller than the one of the surrounding ground (Newmark, 1967; Wang, 1993). Since the soil-structure interaction effects are totally ignored, these methods are commonly referred as 'free-field' analysis methods (Wang, 1993; Hashash et al., 2001). In his pioneer work, Newmark (1967) developed analytical relations for the evaluation of the axial strain and the curvature of a straight buried pipe, neglecting the SPI effects. The relations (Equations 1 and 2), are based on the assumption that a straight pipe is embedded in a homogeneous, isotropic, infinite and elastic soil medium, which is subjected to constant plane seismic wave, the latter propagated in parallel with the pipeline axis with a velocity c.

$$\frac{\partial u}{\partial x} = \frac{1}{c} \times \frac{\partial u}{\partial t} \qquad (1)$$

$$\frac{\partial^2 v}{\partial x^2} = \frac{1}{c^2} \times \frac{\partial^2 v}{\partial t^2} \qquad (2)$$

The above relations may be used to compute the axial strain and curvature that are imposed on the pipeline, as a result of the propagation of any type of seismic wave (*S*-, *P*- or *R*-wave) under any incidence angle. Based on Newmark's approach, St John and Zahrah (1987) presented a series of solutions for the computation of maximum ground axial strains and curvatures caused by various types of seismic waves, which by assumption can directly be used as predictions for the pipe strains. Newmark's approach is recommended by Eurocode 8 (CEN, 2006) for the seismic design and assessment of buried pipelines, as long as the ground is considered stable, elastic and homogeneous. Despite the simplicity of this framework, the 'free-field' methods may be considered inadequate for the design and assessment of 'stiff' pipelines, i.e. pipelines with low radius over thickness (R/t) ratios, like the steel pipelines commonly used in NG applications, as they may render quite conservative results in terms of pipe strains. Additionally, critical damage modes of steel pipelines can not be simulated with these methods, while salient parameters affecting the seismic response and vulnerability of buried steel pipelines, namely the internal pressure, potential geometric imperfections of the pipe walls and the trench soil and soil-pipe interface characteristics, may not be considered. In this context, the implementation of 'free-field' analysis methods in the seismic vulnerability assessment of buried pipelines is considered rather inadequate.

4.2 Analysis methods that consider the soil-pipe interaction phenomena

When the pipeline stiffness is comparable to that of the surrounding ground, SPI phenomena might take place, leading to differences between the pipe and the surrounding ground

movements and hence affecting the pipe response. Some early studies reported a rather favourable effect of SPI on the seismic response of pipelines that were embedded in uniform soil sites (e.g. Hindy and Novak, 1979). Actually, St John and Zahrah (1987) proposed reduction factors on analytical relations that were initially developed for the computation of internal forces of long underground structures (e.g. pipelines, tunnels) neglecting the SPI effects, in order establish relations that account for these effects. However, for buried pipelines crossing heterogeneous soil sites, the consideration of the SPI effects was found to lead to higher responses (Hindy and Novak, 1979).

4.2.1 Beam or shell element pipe models on soil springs

The simplest and most commonly used approach to account for the SPI effects is the *beam-on-nonlinear-Winkler-foundation* (BNWF) model (Figure 6a). In this analysis framework, the pipe is simulated by means of beam elements, whilst discrete nonlinear translational springs and dashpots of appropriate stiffness and damping are used to account for the soil compliance. The latter are actually applied in the three orthogonal directions. In a one-dimensional representation of the SPI interaction problem, the equations of motion of a pipeline, subjected independently to ground displacement time histories $u_g(t)$ and $v_g(t)$, in the transverse horizontal and the axial direction, respectively, are given as:

$$m\frac{\partial^2 u}{\partial t^2} + c_h\frac{\partial u_{rel}}{\partial t} + EI\frac{\partial^4 u}{\partial t^4} + k_h u_{rel} = 0 \qquad (3)$$

$$m\frac{\partial^2 v}{\partial t^2} + c_a\frac{\partial v_{rel}}{\partial t} - EA\frac{\partial^2 v}{\partial t^2} + k_a u_{rel} = 0 \qquad (4)$$

where u and v are the time-dependent pipe displacement components in the transverse horizontal and axial direction, m is the distributed mass of the pipe, EI and EA are the flexural and axial stiffnesses of the pipe cross-section, k_h, k_a are the equivalent soil springs constants per unit length of the pipeline in the horizontal transverse and axial directions, c_h and c_a are the equivalent soil dashpots constants per unit length of the pipeline in the horizontal transverse and axial directions and $u_{rel} = u - u_g$, $v_{rel} = v - v_g$. The response of the pipe, in terms of strains may be obtained by solving the above equations in the time domain. BNWF models have been widely used by practitioners for design purposes, as well as by researchers in the framework of studies related to the seismic analysis and design of buried pipelines. For instance, Mavridis and Pitilakis (1996) used a BNWF model to highlight the significant effects of soil-pipe interaction on the axial response of buried pipelines. Nourzadeh and Takada (2013) used a dynamic BNWF model to investigate the response of buried steel NG distribution pipelines under seismically-induced transient ground deformations. Papadopoulos et al. (2015) employed a BNWF model to perform 3D dynamic analyses of a buried steel NG pipeline and investigate the effect of the spatial variability of ground seismic motion on its response. In the latter study, the seismic ground deformation time histories that were imposed on the 3D BNWF model were

actually computed along the pipeline length via a separate 2D visco-elastic soil response analysis of the examined soil site.

Since dynamic SSI effects can be ignored in case of buried pipelines, the above equations degenerate to the following quasi-type forms:

$$EI\frac{\partial^4 u}{\partial t^4} = k_h \times \left(u_g - u\right) \qquad (5)$$

$$EA\frac{\partial^2 v}{\partial t^2} = k_a \times \left(v_g - v\right) \qquad (6)$$

Evidently, solving the above equations requires a rational selection of the soil springs constants. Several soil spring models have been proposed the last decades on the basis of experimental and numerical studies, to account for the soil compliance on buried pipelines in both the axial and the horizontal transverse directions (O' Rourke M.J. and Wang, 1978; Selvadurai, 1985; El Hmadi and O'Rourke M.J., 1988). Other studies provided relations for the evaluation of the ultimate soil resistance forces to lateral, vertical or oblique pipeline movements (Audibert and Nyman, 1977; Nyman, 1984; O'Rourke M.J. and El Hmadi, 1988; Hsu et al., 2001). A rather detailed summary of these studies may be found in Psyrras and Sextos (2018).

The most commonly used relationships for the computation of soil springs for buried pipelines are those summarized in ALA (2001) guidelines (Table 1). The discrete soil springs are actually defined in four principal directions, i.e. axial, vertical uplifting, vertical bearing and lateral, following Hansen and Christensen (1961) and Trautmann and O'Rourke (1983) and adopt an elasto-plastic bilinear curve to account for the trench soil and soil-pipe interface non linear response. It is worth noticing that these springs are defined for pipelines embedded in a uniform soil deposits.

The simulation of the pipeline as an equivalent beam may lead to a rough estimation of the axial and bending deformations and strains that are imposed on it by seismically-induced transient ground deformations. The pipe material nonlinearity, which is a crucial parameter in the seismic vulnerability assessment, may be considered by means of fibers (Lee et al., 2016; Jahangiri and Shakib, 2018). However, with this simulation approach, it is not possible to replicate accurately potential seismically-induced damage modes, described in the first part of the paper, e.g. local buckling, ovalization etc. Additionally, it is possible to account for the hoop stresses caused by the pressurization of the steel pipeline, which as seen in *Section 3.3*, interact with the axial straining on the pipe during ground seismic shaking, affecting its axial response. Moreover, critical aspects that may affect the axial compressive response of steel NG pipelines, such as the geometric imperfections of the pipe walls, may not be considered. On the contrary, a *shell model* of the pipeline allows for an adequate simulation of various damage modes, as well as for the consideration of most of the salient parameters described in *Section 3*. In this context, several studies have employed shell pipe models in the analysis of the seismic response and vulnerability of pipelines. In the simplest case, the soil-pipe relative movements

may be neglected and therefore the seismic excitation may be directly be applied on the pipeline; in this case the analysis is degenerated in a structural analysis of the shell pipeline. Kouretzis et al. (2006) followed such as simulation approach, in an effort to validate closed-form solutions for the evaluation of strains caused by seismic *S-waves* on steel pipes. A more accurate alternative, includes the consideration of the soil compliance by means of soil springs, the latter being introduced along the perimeter of the shell model (e.g. Figure 6b). As an example, Lee et al. (1984) used an elasto-plastic cylindrical shell model of a pipe to examine its structural stability under seismic wave propagation, simulating the soil compliance by means of soil springs. The springs were introduced only in the normal direction of the pipe, neglecting the SPI effects in the critical axial direction. In an effort to examine thoroughly the parameters under which a buried pipeline, subjected to compressive axial loading, can bifurcate plastically in either beam- or shell model buckling, Yun and Kyriakidis (1990) used both beam models of pipelines with large-deflection kinematics being accounted for, as well as inelastic shell models, with geometric imperfections being considered. The SPI effects in the later case were considered in a similar fashion with Lee et al. (1984), i.e. by means of normal soil springs, disregarding the axial ones.

The extended length of the buried pipelines, in addition to the need for very refined shell meshes in order to capture potential damage modes, such as local buckling failures, are expected to increase considerably the computational cost of this type of analyses compared to the 'classical' BNWF models. A potential solution towards reducing the relevant computation cost is the use of *hybrid models*, similar to the one illustrated schematically in Figure 6c. In this modelling approach, the critical parts of an examined pipeline, e.g. locations where a buried steel pipeline is crossing identified geotechnical discontinuities that may result in an amplified response under transient ground deformations, are modelled in a detailed fashion, by means of shell elements, while the rest pipeline is simulated by means of beam elements. The latter parts are connected rigidity to the detailed shell model parts. The soil compliance is simulated along the whole length of the pipeline by means of soil springs. An example of this simulation approach is provided by Saberi et al. (2013), who used a hybrid beam-shell pipe model to evaluate the response of steel pipe bends.

Regardless of the simulation approach that is used for the pipeline, the determination of impedance functions (e.g. springs and dashpots) for long underground structures, such as buried pipelines, is a quite delicate problem (Pitilakis and Tsinidis, 2014). The few analytical relations that may be found in the literature are defined on the basis of simplified elasto-plastic idealizations of the actual nonlinear soil-pipe response, while they do not account for the soil heterogeneities along the pipeline axis. Moreover, most of the available relations were derived under the assumption of monotonic loading conditions, neglecting the actual cyclic nature of seismic excitation and the hysteretic characteristics of the soil-pipe system. The effect of coupling of the directional components of the relative soil-pipe motion, on the pipeline response and vulnerability, is commonly disregarded by the available soil spring relations.

Along these lines, further investigation is needed towards the proposal of soil springs or macro-elements that could simulate adequately the soil compliance on buried pipelines.

An additional issue of the pipe shell on soil springs models is related with the introduction of local forces on shell elements at the locations of the soil springs. These forces may alter the distribution of stresses and strains on the pipeline wall and even lead to inaccurate buckling responses. This problem might be more intense in case of coarse mesh of the pipeline. Along these lines, particular emphasis should be placed on the appropriate meshing of the pipeline and simulation of soil compliance by means of soil springs.

4.2.2 3D continuum models of the pipe-trench soil system

An alternative method to consider the soil compliance on buried pipelines in a numerical analysis framework is by simulating part of the surrounding ground, as a continuum trench-like model that encloses the buried pipeline. In this framework, the pipeline is simulated by means of shell elements, whilst solid elements are used for the surrounding trench soil. This simulation allows the use of contact elements or sophisticated contact models that may account rigorously for the potential geometrical nonlinear phenomena along the soil-pipe interface during loading, including sliding, or even separation of the pipe from the surrounding trench soil. This analysis approach was used by some researchers to simulate the response of buried pipelines subjected to permanent ground deformations due to faulting (e.g. Vazouras et al., 2010; Vazouras et al., 2012; Vazouras et al., 2015; Vazouras and Karamanos, 2017; Sarvanis et al., 2017).

The use 3D continuum models of the pipe-trench soil system allows for critical parameters that affect the axial response of buried steel NG pipelines, such as the potential geometric imperfections of the pipeline walls, or the internal pressure of the pipeline, to be effectively considered. The main shortfall of this approach is the higher computational cost, compared to that of beam- or shell-on-soil-springs models. Indeed, implementing 3D continuum models in a vulnerability assessment framework of buried NG pipelines under seismically-induced transient ground deformations, is computationally inefficient, particularly in case, where a large number of full dynamic time histories analyses are expected to be conducted within an IDA, multi-stripe or cloud analysis. However, the approach may be applicable in studies, where the effects of transient ground deformations on the response and vulnerability of the buried NG pipelines are investigated in a pseudo-static manner. A representative example is provided by Psyrras and Sextos (2018), who examined the potential of buckling failures of buried steel NG pipelines that cross heterogeneous soil deposits, when subjected to seismically-induced transient ground deformations. The methodology, which is further detailed in Psyrras et al. (2018) and Psyrras et al. (2019), consists of two separate steps. The in-plane ground deformations that are expected to be imposed on the pipeline during ground seismic shaking are initially computed along its axis, via 2D elastic or visco-elastic response analyses of pre-selected soil sites, neglecting the effects by the presence of the pipeline. The researchers

implemented in their analyses the idealized sites discussed above (i.e. sites consisted of two horizontally adjacent soil layers of highly distinct characteristics and stiff soil/rock sites that included a soft alluvial valley of trapezoidal shape in the middle). An 'adequately' long 3D continuum pipe-trench soil model is used in a second step to evaluate the pipeline response under critical soil displacement patterns, identified from the soil response analyses. The pipe model is simulated by shell elements and is encased by a near-field trench-like soil continuum model. According to the researchers, a trench soil model of reduced dimensions around the pipe, starting from a few meters below the ditch line and reaching up to the ground level, suffices for the proper simulation of the soil compliance since the typical burial depth of NG pipelines is reduced and the SSI effects on buried pipelines are generally not important (see also *Section 3.1*). In the particular study, the trench soil model was simulated by means of elastic solid elements with equivalent soil properties being assign on them (i.e. soil degraded stiffness), the latter being estimated by the separate 2D soil response analyses of the first step. The displacement patterns are introduced statically on the soil volume and transmitted on the pipeline through the soil-pipe interface, which is simulated by means of advanced interaction models. Based on this analysis framework, Psyrras et al. (2019) reported that under particular circumstances and ground motion characteristics buckling damages may be observed on steel NG pipelines, at locations, where the properties of the surrounding ground change drastically.

Evidently, the pseudo-static simulation of the seismic loading, i.e. the transient ground deformations herein, is computationally more efficient compared to a dynamic simulation in the framework of full time histories analyses. However, an 'adequately long' 3D soil-pipe continuum model is required in order to replicate the actual SPI phenomena, accounting for the 'anchorage' length of the pipeline on the surrounding trench soil and its effect on the transmitted stresses on the pipeline through the soil-pipe interface. Additionally, there is a requirement of fine meshes of the pipe and the trench soil, to adequately resolve the buckling modes of the pipeline, which may potentially be caused by seismically-induced ground deformations on the pipeline. The above aspects reduce the applicability of this analysis approach in seismic vulnerability studies, where a large number of analyses are mandatory, in order to establish rigorous analytical fragility curves. A potential solution is to use continuum models with refined meshes at critical locations (e.g. near the assumed geotechnical discontinuities) and much coarser mesh seeds elsewhere. Even with this meshing strategy, the computational times might be quite significant.

4.2.3 3D hybrid continuum models of the pipe-trench soil system

At the time of writing, the authors of this paper were expending efforts to evaluate the vulnerability of buried steel NG pipelines against local buckling failures, potentially induced by seismic transient ground deformations near geotechnical discontinuities. In the framework of this investigation, a 3D hybrid continuum model of the pipe-trench soil system was developed, which may be generally used in relevant studies for the seismic vulnerability

assessment of buried steel pipelines. More specifically, the study focused on idealized soil-pipe configurations, consisting of a buried steel NG pipeline crossing perpendicularly a vertical geotechnical discontinuity with an abrupt change on the soil properties. The analysis framework, which resembles, to some extent the one of Psyrras et al. (2019), consists of two steps. A 3D trench-like continuum soil model, encasing a cylindrical shell model of the pipeline, is initially developed in ABAQUS (2012), in order to compute the axial compressive response of the pipeline under an increasing level of axial relative ground displacement, caused by vertically propagated *S*-waves near a geotechnical discontinuity. The analysis focuses on the axial ground displacements and disregards the vertical ones that might be observed near geotechnical discontinuities since the former introduce much higher strains on the pipeline. Figure 7 illustrates the typical numerical model layout. The pipeline is simulated by means of inelastic shell elements, while solid elastic elements are used to model the trench soil. The properties of the trench soil elements correspond to average equivalent properties of the soil, estimated via the 1D soil response analyses in the separate analysis step, as described in the ensuing. The distance between the side boundaries of the trench model and the pipe edges is set equal to one pipe diameter, whereas the distance between the pipe invert and the bottom boundary of the trench model is set equal to 1.0 m. Evidently, the distance between the pipe crown and ground surface is defined on the basis of the adopted burial depth of the examined pipeline. The mesh is refined at the middle section of the model, which corresponds to the location, where the properties of the site are supposed to change abruptly, thus resulting in a 'step' on the axial ground deformations imposed on the pipeline during the seismic wave propagation (i.e. δ_u in Figure 7). Typical static boundary conditions are applied at the bounding soil surfaces. In particular, the bottom boundary of the soil model is fixed in the vertical direction, while the side-boundaries of the soil model are fixed in the horizontal direction. The ground surface is set free. An advanced contact model is implemented for simulation of the soil-pipeline interface, with the sliding behaviour being controlled by the classical Coulomb friction model. The length of the 3D pipe-soil trench model is set equal to 20 times the diameter of the pipeline, while nonlinear springs, acting parallel to the pipeline axis, are introduced at both end sides of the pipeline, in order to account for the effect of the infinite pipeline length on the response of the examined pipeline-trench soil configuration. The force-displacement relation of the nonlinear springs is given as follows:

$$F_0 = \begin{cases} \lambda EA\delta_x \quad \text{for} \quad \delta_x \le \dfrac{\tau_{\max}}{k_s} \\ \lambda EA\dfrac{\tau_{\max}}{k_s} + \dfrac{\pi D\tau_{\max}}{m}\left(\sqrt{\left(\lambda\dfrac{\tau_{\max}}{k_s}\right)^2 + 2m\left(\delta_x - \dfrac{\tau_{\max}}{k_s}\right)} - \left(\lambda\dfrac{\tau_{\max}}{k_s}\right)\right) \text{for} \quad \delta_x > \dfrac{\tau_{\max}}{k_s} \end{cases} \tag{7}$$

where:

$$\lambda = \sqrt{\frac{\pi D k_s}{EA}} \qquad (8)$$

$$m = \frac{\pi D \tau_{\max}}{EA} \qquad (9)$$

δ_x is the soil-pipe relative axial movement caused by the relative axial ground deformation δ_u, $\tau_{\max}$ is the maximum shear resistance that develops along the soil-pipe interface, k_s is the shear stiffness of the soil-pipe interface and EA is the axial stiffness of the pipeline cross section. As already discussed, for cohesionless backfills, i.e. common trench soil conditions, the maximum shear resistance depends on the adopted Coulomb friction coefficient μ and varies along the perimeter of the pipe. On this basis, mean values of $\tau_{\max}$ and k_s should be computed, based on numerical simulations of simple axial pull-out tests of the examined pipe from the trench soil. It is worth noting that the proposed simulation of the end-boundaries of the pipeline is inspired from a numerical model that was developed by Vazouras et al. (2015), in order to account for the effect of the infinite length of buried pipeline when subjected to seismically-induced strike-slip faulting. The theoretical background and the necessary modifications that are required in order to expand such a simulation approach in case of seismically-induced in-plane transient ground deformations are presented in Appendix A. The selection of the length of the 3D hybrid model is made on the basis of a sensitivity analysis, by comparing the stresses and strains computed at the middle critical section of the pipeline by the 3D hybrid model, with relevant predictions of an equivalent quite extended, almost 'infinite', 3D continuum model of the soil-pipe configuration subjected to the same axial ground deformation pattern. With reference to the loading pattern of the 3D hybrid model; the stress state, associated with the gravity and the internal pressure of the pipeline, is initially established within a general static step. The selected ground displacement pattern is then introduced monotonically on the soil-pipeline configuration, through the soil volume and the free ends of the nonlinear springs, in stepwise ramp-type fashion, as per Figure 7. This loading condition results in an axial compressive response of the pipeline, which may be traced for an increasing level of relative axial displacement δ_u through a simple static analysis step or even better via a modified Riks solution algorithm. Through this analysis, a correlation between the relative axial ground displacement δ_u and the maximum compressive axial strain of the critical middle section of the pipeline (i.e. near the assumed geotechnical discontinuity) may be established.

In a second step, critical relative axial ground deformation patterns δ_{ue} are determined at the pipeline's depth, for selected sites, consisting of two laterally adjacent soil deposits of dissimilar properties, subjected to ground seismic motions at their base, in the form of vertically propagated *S*-waves. A series of separate 1D nonlinear soil response analyses of the adjacent soil deposits are carried out for this purpose, under a variety of selected ground seismic motions, in the framework of an IDA, multiple-stripe or cloud analysis. The outcome of the soil response analyses, in terms of critical relative axial ground deformation patterns δ_{ue}

and various seismic *IMs* at the burial depth of the pipeline or at bedrock conditions, is finally correlated with the predicted straining of the pipeline, using the δ_u - maximum compressive axial strain correlations computed by the 3D SPI analyses in the first step.

Since the response of the pipeline is computed for an increasing level of relative axial ground displacement δ_u, the outcome of one 3D SPI analysis can be used to examine the axial straining of the pipe under a variety of selected ground axial relative displacements δ_{ue}, caused by diverse ground seismic motions. This of course is possible under the assumption and implementation of mean equivalent soil properties for the trench-soil, corresponding to the strain-range that is anticipated by the selected ground seismic motions. The mean equivalent soil properties (i.e. degraded soil stiffness) are actually estimated for the examined range of strains, which are caused by the selected ground motions, via the 1D soil response analyses. Additionally, with this analysis approach, crucial parameters that affect the axial response of pipelines under compression, such as the initial geometric imperfections of the pipeline walls or the level of internal pressure of the pipeline, can effectively be considered.

Figure 8 illustrates some representative results from 3D SPI analyses that were carried out following the first step of the above analysis framework. In particular, contour diagrams of the axial stresses, developed at the critical zone of the pipeline (i.e. the middle zone of the pipeline model, where the soil properties are assumed to change), are plotted for two distinct steps of the analysis, i.e. before major concentration of stresses and buckling failure at the zone and at the end of the analysis, after buckling failure occurrence. The diagrams are plotted on the deformed shapes of the pipelines, so as to highlight the buckling failures that occur for higher levels of imposed relative axial ground deformations. Additionally, the figure portrays the evolution of maximum compressive strain of the critical pipeline zone with increasing relative axial ground deformation δ_u. The presented results correspond to a steel API 5L X65 pipeline with diameter D = 762 mm and wall thickness t = 14.3 mm (i.e. R/t = 26.6), which is embedded 1 m bellow the ground surface, in a trench soil with density, ρ = 1.65 t/m^3, shear modulus G = 37 MPa and Poisson ratio, ν = 0.3 (trench soil A). A friction coefficient μ = 0.45 is considered at the soil-pipe interface, while the nonlinear springs at the end-sides of the pipe are defined, as per Equation 7. The results are provided for various levels of internal pressure for the pipeline (i.e. p = 0, 4 MPa and 8 MPa), while both a 'perfect' and an equivalent imperfect pipeline are considered. For the simulation of the imperfect pipeline, a stress-free, biased axisymmetric imperfection is considered, having maximum amplitude of 10 % of the pipe wall thickness. It is recalled herein that the level of imperfection is based on relevant specifications from NG pipeline manufactures, e.g. ArcelorMittal (2018). This imperfection is applied over a short zone of 2.0 m, centred at the middle of the pipeline model.

In line with the previous observations, both the pressurization level of the pipeline and the initial geometric imperfections affect the axial response of the examined pipelines. In particular, with increasing relative axial ground deformation δ_u, the pipeline tends to bend upwards, i.e. towards the free ground surface. This response results in an early concentration of

compressive axial stresses at the invert part of the pipeline. The existence of geometric imperfections is found to affect significantly the distribution of the axial stresses on the pipeline. Actually, these stresses tend to distribute more uniformly across the lower part of the perfect pipeline. On the contrary concentrations of stresses are observed at the imperfection 'bulges' of the imperfect pipeline. The pressure level of the pipeline tends to affect the buckling patterns of the pipelines that take place under increased relative axial ground deformations, i.e. $\delta_u \approx 14-20cm$ for the examined cases. Inward deformations of the pipe walls (i.e. deformations towards the pipe cavity) are observed for the non-pressurized (i.e. p = 0 MPa) or the low pressurized (i.e. p = 4 MPa) pipelines, while a combination of inward and outward deformations (i.e. deformations towards the trench soil) are observed on the highly pressurized pipelines (i.e. p = 8 MPa). The effects of the above parameters are evident on the evolution of maximum compressive axial strain of the critical zone of the pipeline with the increasing relative axial ground deformation δ_u. Higher stains are reported on the pressurized pipelines even at low δ_u, compared to those predicted on the non-pressures pipelines. This observation is related to the combining effect of the internal pressure and the axial compressive straining of the pipeline caused by the ground movement, on axial response of the pipeline (see also *Section 3.3*). Additionally, the pipeline with the geometric imperfection tends to concentrate higher strains throughout the analysis compared to the equivalent 'perfect' pipeline, with the differences between the two cases being as high as 15 %.

Similar comparisons of the computed axial response of the examined pipelines are presented in Figure 9, referring to the case where the pipelines are embedded in a stiffer trench soil (density, ρ = 1.9 t/m^3, shear modulus G = 63 MPa, trench soil B) with a higher soil-pipe friction coefficient be also considered, i.e. μ = 0.78. The examined pipelines exhibit a higher axial response, both in terms of axial stresses and axial strains, compared to the previous case (i.e. for trench soil A), with the buckling phenomena taking place in lower relative axial ground deformations, i.e. $\delta_u \approx 8-10cm$. This increasing axial response is attributed to the higher axial deformations that are transferred from the trench to the pipeline through the rougher interface. Additionally, the higher confinement that is being offered by the surrounding trench soil partially reduces the upward bending of the pipeline (i.e. bending towards the ground surface) during the kinematic loading of the system, which in turn leads to an increased localization of axial straining at the critical zone of the pipeline.

Inevitably, there are some limitations with the analytical methodology described herein. The effect of inertial SPI and of the evolution of stresses and deformations on the pipeline response, as well as time-dependent phenomena, such as fatigue and steel strength and stiffness degradation due to cyclic loading, are all neglected.

4.3 Summary and identified challenges

The selection of a suitable methodology to evaluate the vulnerability of buried steel NG pipelines against seismically-induced transient ground deformations, depends largely on the damage mechanism of interest, as well as the desired degree of accuracy, since the physical problem in its entirety is extremely complex and uncertain (Psyrras and Sextos, 2018). Theoretically, detailed full dynamic analysis, making use of 3D numerical models of the soil-pipe configuration and accounting for the material nonlinearities of the soil and the pipe, as well as for the geometric nonlinearities that might take place along the soil-pipe interface, constitute the most rigorous way to evaluate the seismic response and vulnerability of buried steel pipelines. However, the very large dimensions of the problem, the complexity of simulating material and geometrical nonlinearities and the geometric imperfections of the pipelines, the uncertainties in the definition of the characteristics of heterogeneous soil sites and the inherently random varying ground seismic motion, render a fully 3D time history analysis of the coupled pipeline-trench soil system computationally prohibitive. Along these lines, some simplifications should always be made. Table 2 summarizes the most important advantages and disadvantages of the presented 'simplified' methods, along with their potential applicability for design or vulnerability assessment purposes.

'Free-field' analysis methods may be considered inadequate for the seismic vulnerability assessment of buried steel NG pipelines since they can not be used for the simulation of distinct damage modes, while they may not account for salient parameters controlling the seismic response of buried steel pipelines. Simplified BNWF models have been proposed in the literature to account for the effects of SPI on the seismic response and vulnerability of buried pipelines. The simulation of the pipeline as an equivalent beam may result in a rough estimation of the axial and bending deformations and strains. However, this analysis approach does not allow for an accurate simulation of diverse damage modes of buried steel NG pipelines, while again it is not possible to account for all the important parameters that might affect the axial response of this infrastructure. The alternative use of shell-pipe models on soil springs may be helpful towards a better simulation of critical damage modes of buried steel pipelines. However, the accurate evaluation of the soil springs is a rather delicate problem that remains still open. Moreover, the adequate meshing of the pipeline with shell elements is a very important issue that should always be carefully accounted for.

The simulation of the soil compliance by means of a continuum model, enclosing the buried pipeline, constitutes an alternative analysis approach. This type of SPI models, in combination with a pseudo-static simulation of the seismically-induced transient ground deformations, may provide a rather rigorous framework for the vulnerability assessment of buried steel NG pipelines. This approach requires a series of separate soil response analysis to determine critical soil displacement patterns that are used as input for the SPI analysis models. Obviously, this analysis framework is associated with a higher computational cost compared to that of beam- or shell-on-soil-spring models. An alternative to the later simulation approach, which

makes use of nonlinear springs to reduce the required length of the detailed 3D SPI models, while accounting for the effect of pipeline infinite length, i.e. the 3D hybrid models, was presented above. The method may account for critical parameters affecting the seismic response and vulnerability of steel buried NG pipelines, while reducing significantly the associated computational cost.

Regardless of the selected methodology, the 'accurate' simulation of the site conditions, as well as the consideration of salient parameters affecting the pipeline axial response, are expected to lead to more reliable observations regarding the seismic response of buried NG pipelines, contributing towards the selection of the optimum seismic *IM* for each damage mode and the development of reliable analytical fragility functions to be used in quantitative risk assessment of NG networks.

The validation of the above methodologies against experimental results from rigorous test campaigns or data from real cases in the field may provide evidence on the efficiency of each analysis approach. A series of shaking table tests were recently carried out on a pipeline model, embedded in an inhomogeneous soil site, at the shaking table of the University of Bristol, in the framework of the Exchange-RISK project (http://www.exchange-risk.eu/). One of the novelties of this testing campaign was the recording of the strains across the pipeline by means of distributed fiber optic sensing. The results of this study are expected to shed light on seismic response of buried pipelines that are embedded in similar soil sites, while they will constitute a valuable dataset for validating the relevant analysis approaches.

5. Conclusions

Alternative analytical methods for the evaluation of the vulnerability of buried steel NG pipelines under seismically-induced transient ground deformations were thoroughly presented in this part of the paper. Particular emphasis was placed on the analytical tools for the vulnerability assessment against seismically-induced buckling failure modes since these constitute critical damage modes for the structural integrity of buried steel pipelines. Salient parameters that control the seismic response and vulnerability of buried steel pipelines and therefore should be considered in the relevant analytical methods were discussed, while a new analysis approach for the assessment of buried steel NG pipelines was also introduced. The main conclusions of this study may be summarized as follows:

- The seismic response and vulnerability of buried steel NG pipelines is dominated by the kinematic loading induced by the seismic movement of the surrounding ground. This mechanism is actually causing the axial or bending straining on the pipeline, which in turn may lead to distinct damage failures. The geologic and geotechnical conditions of the site, the distance of the site from the seismic source, the internal pressure of the pipeline, the potential geometric imperfections of the walls of the pipeline, the characteristics of the trench soil, any potential restrictions of the pipeline (e.g. elbows), as well as the spatial variation of the ground seismic motion along the pipeline axis, are among the parameters

that may affect the axial response of a buried steel NG pipeline caused by seismically-induced transient ground deformations. Along these lines, the above parameters should be considered to the highest level possible by the numerical approaches that are implemented for analytical evaluation the seismic vulnerability of this critical civil infrastructure.

- The complexity of the seismic response and vulnerability of buried steel NG pipelines, in addition to the high level of uncertainty on the definition of the above parameters, renders the use of a 3D full dynamic time history analysis computationally prohibitive, particularly in the framework of a seismic vulnerability analysis. Hence, the use of simplified models in vulnerability assessment studies of NG pipeline networks is inevitable. BNWF models, shell pipe models on soil springs or hybrid shell-beam pipe models on soil springs may be used in the framework of dynamic time history analysis or pseudo-static analyses for the vulnerability assessment of buried steel NG pipelines. These approaches offer computational efficiency. The main shortcoming of the above analytical models is related with the simulation of the soil compliance on the pipeline via 'simplified' soil springs. A The use of 3D pipe-trench soil continuum models, combined with a pseudo-static simulation of the seismically-induced transient ground deformations, computed separately by means of a soil response analysis, may provide a more rigorous framework for the vulnerability assessment of buried steel NG pipelines. The latter framework is associated with a higher computational cost compared to that of a beam- or shell-on-soil-springs models. However, this shortcoming may be partially resolved through the use of hybrid boundaries at the end-sides of the pipe, so as to reduce the required length of the 3D derailed model and the relevant computational cost, whist accounting for the effect of the pipeline infinite length in an efficient fashion. Regardless of the selected analysis approach, the validation of numerical tools with experimental data from rigorous testing campaigns or recordings from real case studies, may contribute towards more reliable analysis frameworks for the quantitative vulnerability assessment of buried steel NG pipelines.

Appendix A. Nonlinear springs for the simulation of an infinitely long pipeline subjected to axial loading due to seismically-induced in-plane relative axial ground deformations near geotechnical discontinuities

This appendix summarizes the theoretical background for the definition of the nonlinear springs that are introduced at the end-boundaries of the detailed 3D SPI hybrid model, in order to account for the effect of the infinite length of a buried pipeline, subjected to seismically-induced in-plane relative axial ground deformations near a geotechnical discontinuity, on its axial response. The proposed simulation is inspired by a numerical model that was developed by Vazouras et al. (2015) to account for the infinite length of buried pipeline when subjected to seismically-induced strike-slip faulting. Given the differences between the two loading

mechanisms, some modifications are required in order to expand such a simulation approach herein.

Figure A1 illustrates schematically the problem in hand. Only the right-hand side end boundary of the hybrid SPI model is presented and discussed herein. A similar approach should be followed for the left-hand side end boundary of the model. An infinitely long buried steel NG pipeline of diameter D is considered to be embedded in a uniform elastic trench soil of density ρ, Young's modulus, E_s, and Poisson's Ratio, v_s. The pipeline is made of steel, having a Young's Modulus, E, and Poisson's Ratio, v. The trench soil volume, surrounding the pipe, is subjected to a seismically-induced in-plane transient ground deformation, which is introduced on the trench soil in a pseudo-static manner and corresponds to the maximum ground deformation computed at the site of interested during ground seismic shaking from a separated soil response analysis. This deformation is kept constant with the depth coordinate over the trench soil domain, on the grounds that the depth of the truncated domain is small compared to the maximum predominant wavelength of the impinging waves examined, hence the in-plane motion of the soil particles does not vary significantly in depth (Psyrras et al., 2019). The deformation yields in a uniform movement of the trench-soil parallel to the pipeline axis, i.e. u_s in Figure A1. The soil movement mobilizes shear stresses along the soil-pipe interface, which cause compressive or tensile axial deformations on the pipeline, i.e. u_p in Figure A1.

The shear stresses that are critical for the development of the axial deformations on the pipeline are largely depending on the tangential behaviour of the soil-pipe interface, which is assumed to follow the elasto-plastic law, as per Figure A2. The latter is defined on the basis of the shear stiffness k_s and maximum shear resistance τ_{max} of the soil-pipe interface. For cohesionless soils, which constitute a common backfill for trenches of pipelines, the above parameter may be evaluated via a simple pull-out analysis of the pipeline from the trench soil (Figure A2), as per Vazouras et al. (2015).

When the soil movement u_s is higher than a critical value, sliding will occur on part of the soil-pipe interface, i.e. along the sliding segment of the pipeline of length L_s, in Figure A1, while the rest length of the infinite pipe will remain fully bonded to the surrounding ground, i.e. the fixed segment of the pipeline, of length L_e in Figure A1.

For very low relative pipe-trench soil displacements, the pipeline may be considered full bonded with the surrounding trench soil and the shear stresses developed along the perimeter of the pipeline that are lower the maximum shear resistance τ_{max} and may be computed as follows:

$$\tau = k_s u \qquad \text{(A1)}$$

where u is the relative displacement on the pipe-soil interface caused by the soil movement u_s and the pipe movement u_p. Considering the stress-strain relationship of the pipe material and the axial force equilibrium, the equilibrium equation for the pipe segment yields into:

$$\frac{d^2u}{dx^2} - \lambda^2 u = 0 \qquad \text{(A2)}$$

where:

$$\lambda^2 = \frac{\pi D k_s}{EA} \qquad \text{(A3)}$$

Accounting for the particular boundary conditions of the problem herein, the solution of Equation A2 is given by the following equation:

$$u(x) = ue^{-\lambda x} \qquad \text{(A4)}$$

The corresponding axial force along the pipe may then be evaluated as follows:

$$F(x) = -EA\varepsilon = -EA\frac{du}{dx} = \lambda EAue^{-\lambda x} \qquad \text{(A5)}$$

For the limit case, at which sliding initiates at $x = 0$, i.e. at the end boundary of the hybrid model, the relative displacement $u(0) = \delta_x = u_s - u_p$ becomes equal to the elastic slip displacement $u_e = \tau_{\max}/k_s$; hence, Equation A5 yields:

$$F_0 = \lambda EA\frac{\tau_{\max}}{k_s} \qquad \text{(A6)}$$

When the relative soil-pipe displacement is higher than the elastic slip displacement, then sliding occurs along a part of the pipeline, i.e. sliding segment of length L_s in Figure A1, while the rest of soil-pipeline interface is responding elastically, exhibiting no sliding. It can be shown that the equilibrium equation for the sliding segment is given by the following expression:

$$EA\frac{d^2u}{dx^2} - \pi D\tau_{\max} = 0 \rightarrow \frac{d^2u}{dx^2} - m = 0 \qquad \text{(A7)}$$

where

$$m = \frac{\pi D\tau_{\max}}{EA} \qquad \text{(A8)}$$

Considering the distribution of the pipeline axial strain along its axis due to the assumed kinematic loading, as well as the boundary conditions of the problem in hand, it can be shown that the length of the pipe, along which sliding occurs, is given by the following expression:

$$L_s = \frac{1}{m}\left(\sqrt{\left(\lambda\frac{\tau_{\max}}{k_s}\right)^2 + 2m\left(\delta_x - \frac{\tau_{\max}}{k_s}\right)} - \left(\lambda\frac{\tau_{\max}}{k_s}\right)\right) \qquad \text{(A9)}$$

Finally, the force at the end-boundary of the 3D SPI hybrid model, caused by the relative displacement between the soil and the pipe is:

$$F_0 = \pi D\tau_{\max}L_s + \lambda EA\frac{\tau_{\max}}{k_s} \qquad \text{(A10)}$$

Summarizing, the force-displacement relation of the nonlinear spring that replicates the effect of an infinite long pipe is given by the following expressions:

$$F_0 = \begin{cases} \lambda EA\delta_x \quad \text{for} \quad \delta_x \le \dfrac{\tau_{\max}}{k_s} \\ \lambda EA\dfrac{\tau_{\max}}{k_s} + \dfrac{\pi D\tau_{\max}}{m}\left(\sqrt{\left(\lambda\dfrac{\tau_{\max}}{k_s}\right)^2 + 2m\left(\delta_x - \dfrac{\tau_{\max}}{k_s}\right)} - \left(\lambda\dfrac{\tau_{\max}}{k_s}\right)\right) \text{for} \quad \delta_x > \dfrac{\tau_{\max}}{k_s} \end{cases} \tag{A11}$$

The above relations and assumptions are valid for both tensile and compression axial loading of the pipeline, caused by the ground axial movement. From a simulation perspective, to account for the relative deformation δ_x at the side boundaries of the pipeline of the hybrid model, one should introduce the ground deformation u_s pattern on both the volume of the trench soil, as well as on the free end of the nonlinear springs (as per Figures 7 and A1). This is the only actual modification of this simulation approach, compared to Vazouras et al. (2015). The length of the detailed 3D SPI model should be selected on the basis of a short parametric analysis, preceded the vulnerability analysis study. Generally, the length of the model should be long enough, to avoid any bias of the results caused by potential boundary effects, and at the same time, short enough, to avoid a misrepresentation of the actual kinematic loading induced by the surrounding trench soil.

The above simulation approach is validated for a representative pipe-trench soil configuration in the following, by comparing the results of the 3D hybrid SPI model, in terms of pipeline Mises stresses and axial strains at the critical middle section of the pipeline (i.e. where soil properties and hence ground deformation are changed), with the predictions of an equivalent 'infinitely' long 3D detailed model of the examined system. The comparisons refer to an API-X65 steel NG pipeline with outer diameter D = 914 mm (36 in), wall thickness t =12.7 mm (i.e. radius over thickness ratio, R/t=36), yield strength σ_y = 448.5 MPa, Young's modulus E = 210 GPa and Poisson's ratio, ν = 0.3. The pipeline is pressurized to a pressure level of 8 MPa and is assumed to be embedded at burial depth of 1 m below the ground surface in a trench soil, characterized by a density ρ = 1.65 t/m^3, a Young's modulus E = 42.9 MPa, and a Poisson's ratio, ν = 0.3. The length of the 3D hybrid SPI model is set equal to 20 times the diameter of the pipeline, with the end boundaries being simulated by means of nonlinear springs, as per Equations A11. The length of the long 'infinite' model was set equal to 1000 D, to ensure that its predictions were approaching those of a numerical model with infinite length. Figure A3 compares contour diagrams of the Mises stresses and axial strains distributions computed at the critical central section of the pipeline as s result of a relative ground axial deformation δ_u = 20 cm, introduced at the middle of the sections. The comparisons refer to two friction coefficients for the soil-pipe interface, i.e. μ = 0.3 and μ = 0.78. Clearly, for both soil-pipe interface conditions, the 3D hybrid model results in very similar –if not identical – results with the long

3D SPI models, while a higher axial response of the pipeline is naturally reported for the rougher soil-pipe interface.

Acknowledgements

This work was supported by the Horizon 2020 Programme of the European Commission under the MSCA-RISE-2015-691213-EXCHANGE-Risk grant (Experimental and Computational Hybrid Assessment of NG Pipelines Exposed to Seismic Hazard, www.exchange-risk.eu). This support is gratefully acknowledged.

References

ABAQUS, 2012. ABAQUS: theory and analysis user's manual version 6.12. Providence, RI, USA: Dassault Systemes Simulia.

American Lifelines Alliance. 2001a. Seismic fragility formulations for water systems. Part 1- Guidelines. ASCE-FEMA, Washington, DC, USA.

ArcelorMittal (2018) High yield SAW welded Pipe API 5L grade X65 PSL 2. 65:5-6.

American Lifelines Alliance., 2001b. Seismic fragility formulations for water systems. Part 2 - Appendices. ASCE-FEMA, Washington, DC, USA.

Audibert, J.M.E., Nyman, K.J., 1977. Soil restraint against horizontal motion of pipes. Journal of the Geotechnical Engineering Division. 103(10), 1119-1142.

Bakalis K, Vamvatsikos D. (2018) Seismic fragility functions via nonlinear response history analysis. ASCE Journal of Structural Engineering. 144(10):04018181.

Chaloulos, Y.K., Bouckovalas, G.D., Zervos, S.D., Zampas, A.L., 2015. Lateral soil-pipeline interaction in sand backfill: Effect of trench dimensions. Computers and Geotechnics. 69, 442-451.

Chaloulos, Y.K., Bouckovalas, G.D., Karamitros, D.K., 2017. Trench effects on lateral p-y relations for pipelines embedded in stiff soils and rocks. Computers and Geotechnics. 83, 52-63.

Datta, T.K., 1999. Seismic response of buried pipelines: A State-of-the-art review. Nuclear Engineering and Design, 192(2-3), 271-284.

El Hmadi, K., O'Rourke, M., 1988. Soil springs for buried pipeline axial motion. Journal of Geotechnical Engineering, 114(11):1335-1339.

European Committee for Standardization (CEN), 2006. EN 1998-4: 2006. Eurocode 8: Design of structures for earthquake resistance-Part 4: Silos, tanks and pipelines. European Committee for Standardization, Brussels.

FHWA (Federal Highway Administration), 2009. Technical manual for design and construction of road tunnels-Civil elements. Publication No. FHWA-NHI-10-034, Department of transportation, Federal Highway Administration, Washington D.C., U.S.

Gelagoti, F., Kourkoulis, R., Anastasopoulos, I., Tazoh, T., Gazetas, G. Seismic wave propagation in a very soft alluvial valley: Sensitivity to ground-motion details and soil nonlinearity, and generation of a parasitic vertical component. Bulletin of Seismological Society of America. 100, 3035-3054.

Hamada, M., O'Rourke, T.D., Yoshizaki, K., 2000. Large deformation behavior of low-angle pipeline elbows subjected to in-plane bending. In proceedings of the 12th World Conference of Earthquake Engineering, Auckland, New Zealand, 2000. Paper No.:1-8.

Hansen, J.B., Christensen, N.H., 1961. The ultimate resistance of rigid piles against transversal forces. Copenhagen: Geoteknisk Institut.

Hashash, Y.M.A., Hook, J.J., Schmidt, B., Yao, J.I.-C., 2001. Seismic design and analysis of underground structures. Tunnelling and Underground and Space Technology. 16 (2), 247-293.

Hindy, A., Novak, M., 1979. Earthquake response of underground pipelines. Earthquake Engineering and Structural Dynamics. 7:451-476.

Hsu, T., Chen, Y., Wu, C., 2001. Soil friction restraint of oblique pipelines in loose sand. Journal of Transportation Engineering, ASCE, 127(1)82-87.

ISO (International Organization for Standardization), 2005. ISO 23469: Bases for design of structures - Seismic actions for designing geotechnical works. International Standard ISO TC98/SC3/WG10. Geneva, Switzerland: International Organization for Standardization.

Jahangiri, V., Shakib, H., 2018. Seismic risk assessment of buried steel gas pipelines under seismic wave propagation based on fragility analysis. Bulletin of Earthquake Engineering.16(3), 1571-1605.

Jalayer, F., Cornell, C.A., 2009. Alternative non-linear demand estimation methods for probability-based seismic assessments. Earthquake Engineering and Structural Dynamics. 38(8), 951-972.

Jalayer, F., De Risi, R., Manfredi, G., 2015. Bayesian cloud analysis: efficient structural fragility assessment using linear regression. Bulletin of Earthquake Engineering. 13(4), 1183-1203.

Jalayer F, Ebrahimian H, Miano A, Manfredi G, Sezen H. 2017. Analytical fragility assessment using unscaled ground motion records. Earthquake Engineering and Structural Dynamics, 1–25.

Karamanos, S.A., 2016. Mechanical behavior of steel pipe bends: An overview. Journal of Pressure Vessel Technology of the ASME, 138(4), 041203.

Karamitros, D.K., Zoupantis, C., Bouckovalas, G.D., 2016. Buried pipelines with bends : analytical verification against permanent ground displacements. Canadian Geotechnical Journal. 53(11), 1782-1793.

Katsumi, M., Masaru, H., 2000. Soil spring constants of buried pipelines for seismic design. Journal of Engineering Mechanics. 126(1), 76-83.

Kouretzis, G.P., Bouckovalas, G.D., Gantes, C.J., 2006. 3-D shell analysis of cylindrical underground structures under seismic shear (S) wave action. Soil Dynamics and Earthquake Engineering. 26, 909-921.

Kouretzis, G.P., Sheng, D., Sloan, S.W., 2013. Sand-pipeline-trench lateral interaction effects for shallow buried pipelines. Computers and Geotechnics. 54:53-59.

Kyriakides, S., Corona, E., 2007. Plastic buckling and collapse under axial compression. Mechanical Offshore pipelines buckling collapse. 1, 280-318, Elsevier Science, New York.

Lanzano, G., Bilotta, E., Russo, G., Silvestri, F., 2015. Experimental and numerical study on circular tunnels under seismic loading. European Journal of Environmental and Civil Engineering 19 (5), 539-563.

Lee, D.H., Kim, B.H., Jeong, S.H., Jeon, J.S., Lee, T.H., 2016. Seismic fragility analysis of a buried gas pipeline based on nonlinear time-history analysis. International Journal of Steel Structures. 16(1), 231-242.

Lee, D.-H., Kim, B.-H.B.H., Lee, H., Kong, J.-S.J.S., 2009. Seismic behavior of a buried gas pipeline under earthquake excitations. Engineering Structures. 31,1011-1123.

Lee, L.N.H., Ariman, T., Chen, C.C., 1984. Elastic-plastic buckling of buried pipelines by seismic excitation. International Journal of Soil Dynamics and Earthquake Engineering. 3, 168-173.

Liang, J., 1995. 3-D Seismic response of pipelines through multiple soil media. Journal of Pressure Vessel Pipelines, 312, 101-107.

Mavridis, G.A., Pitilakis, K.D., 1996. Axial and transverse seismic analysis of buried pipelines. In proceedings of the Eleventh World Conference on Earthquake Engineering, Mexico, 1996.

NASA, 1968. Bucking of Thin Walled Circular Cylinders. NASA SP-8007, doi:19690013955.

Newmark, N.M., 1967. Problems in wave propagation in soil and rocks. Proceeding of International Symposium on Wave Propagation and Dynamic Properties of Earth Materials, University of New Mexico Press, 7-26.

Nishio, N., Ishita, O., Tsukamoto, K., 1983. Model experiments on the behavior of buried pipelines during earthquakes. American Society of Mechanical Engineers, Pressure Vessels Piping Division. PVP-77. In proceedings of the American Society of Mechanical Engineers Pressure Vessel and Piping Conference, Portland, OR, USA.

Nourzadeh, D., S. T., 2013. Response of gas distribution pipelines network to seismic wave propagation in Greater Tehran Area, Iran. In the Proceedings of the 6th China-Japan-US Trilateral Symposium Lifeline Earthquake Engineering, 237-244.

Nyman, K., 1984. Soil response against oblique motion of pipes. Journal of Transportation Engineering. 110(2), 190-202.

Miano A, Jalayer F, Ebrahimian H, Prota A. (2018) Cloud to IDA: Efficient fragility assessment with limited scaling. Earthquake Engineering and Structural Dynamics, 47:1124–1147.

O'Rourke, M.J., Wang, L.R.L., 1978. Earthquake response of buried pipelines. Proceedings of the ASCE Geotechnical Engineering Division Specialty Conference, June 19-21, 1978, Pasadena, California. 720–731.

O'Rourke, M.J., Hmadi, K., 1988. Analysis of continuous buried pipelines for seismic wave effects. Earthquake Engineering and Structural Dynamics. 16, 917-929.

Papadopoulos, S.P., Sextos, A.G., Kwon, O.-S., Gerasimidis, S., Deodatis, G., 2017. Impact of spatial variability of earthquake ground motion on seismic demand to natural gas transmission pipelines. In the Proceedings of the 16th World Conference on Earthquake Engineering. Santiago, Chile, 9-13 January; 2017.

Paquette, J.A., Kyriakides, S., 2006. Plastic buckling of tubes under axial compression and internal pressure. International Journal of Mechanical Sciences. 48, 855-867.

Pitilakis, K., Tsinidis, G., 2014. Performance and seismic design of underground structures, in: Maugeri, M., Soccodato, C. (Eeds.), Earthquake geotechnical engineering design, Geotechnical Geological and Earthquake Engineering 28. Springer international publishing, Switzerland, pp. 279-340.

Psyrras N. and Sextos A., 2018. Safety of buried steel natural gas pipelines under earthquake-induced ground shaking: A review. Soil Dynamics and Earthquake Engineering. 106, 254-277.

Psyrras, N., Kwon, O., Gerasimidis, S., Sextos, A., 2018. Safety factors of buried steel natural gas pipelines under spatially variable earthquake ground motion. In proceedings of the 11th U.S. National Conference on Earthquake Engineering, Los Angeles, California.

Psyrras, N., Kwon, O., Gerasimidis, S., Sextos, A., 2019. Can a buried gas pipeline experience local buckling during earthquake ground shaking? Soil Dynamics and Earthquake Engineering. 116, 511-529.

Riga, E., Makra, K., Pitilakis, K., 2018. Investigation of the effects of sediments inhomogeneity and nonlinearity on aggravation factors for sedimentary basins. Soil Dynamics and Earthquake Engineering. 110, 284-299.

Saberi, M., Behnamfar, F., Vafaeian, M., 2013. A semi-analytical model for estimating seismic behavior of buried steel pipes at bend point under propagating waves. Bulletin of Earthquake Engineering. 11:1373-1402.

Scandella, L., Paolucci, R., 2010. Earthquake induced ground strains in the presence of strong lateral soil heterogeneities. Bulletin of Earthquake Engineering. 8, 1527–1546.

Selvadurai, A.P.S., 1985. Soil-pipeline interaction during ground movement. Civil Engineering in the Arctic Offshore. American Society of Civil Engineers, New York, N.Y.

Sextos, A.G., Pitilakis, K.D., Kappos, A.J., 2003. Inelastic dynamic analysis of RC bridges accounting for spatial variability of ground motion, site effects and soil-structure interaction phenomena. Part 1: methodology and analytical tools. Earthquake Engineering and Structural Dynamics. 32:607-627.

Sextos, A.G., Kappos, A.J., 2009. Evaluation of seismic response of bridges under asynchronous excitation and comparisons with Eurocode 8-2 provisions. Bulletin of Earthquake Engineering. 7, 519–545.

Shinozuka, M., Koike, T., 1979. Estimation of structural strains in underground lifeline pipes.

St. John, C.M., Zahrah, T.F., 1987. Aseismic design of underground structures. Tunnelling and Underground Space Technology. 2(2), 165-197.

Timoshenko, S.P., Gere, J.M., 1961. Theory of elastic stability. McGraw-Hill.

Trautmann, C.H., O'Rourke, T.D., 1983. Behavior of pipe in dry sand under lateral and uplift loading. School of Civil and Environmental Engineering, Cornell University, Ithaca, N.Y.

Trautmann, C.H., O'Rourke, T.D., 1985. Lateral force-displacement response of buried pipe. Journal of Geotechnical Engineering. 111(9), 1077-1092.

Tsinidis, G., Pitilakis, K., Madabhushi, G., Heron, C., 2015. Dynamic response of flexible square tunnels: centrifuge testing and validation of existing design methodologies. Geotechnique. 65 (5), 401-417.

Tsinidis, G., Pitilakis, K., Madabhushi, G., 2016a. On the dynamic response of square tunnels in sand. Engineering Structures. 125, 419-437.

Tsinidis, G., Rovithis, E., Pitilakis, K., Chazelas, J.L., 2016b. Seismic response of box-type tunnels in soft soil: Experimental and numerical investigation. Tunnelling and Underground Space Technology. 59, 199-214.

Tsinidis G., Pitilakis K., Anagnostopoulos, C., 2016c. Circular tunnels in sand: dynamic response and efficiency of seismic analysis methods at extreme lining flexibilities. Bulletin of Earthquake Engineering, 14(10), 2903-2929.

Tsinidis, G., Di Sarno, L., Sextos, A., Psyrras, N., Furtner, P., 2018. On the numerical simulation of the response of gas pipelines under compression. In proceedings of the 9th International Conference on Advances in Steel Structures, ICASS'2018, 5-7 Dec 2018, Hong Kong, China.

Tsinidis, G., Di Sarno, L., Sextos, A., Furtner, P., 2019. A critical review on the vulnerability assessment of natural gas pipelines subjected to seismic wave propagation. Part 1: Fragility relations and implemented seismic intensity measures. Tunnelling and Underground Space Technology, 86, 279-296.

Vamvatsikos, D., and Cornell, C.A., 2002. Applied incremental dynamic analysis. Earthquake Spectra. 202, 523-553.

Yoshizaki, K., O'Rourke, T.D., Hamada, M., 2003. Large scale experiments of buried steel pipelines with elbows subjected to permanent ground deformation. Structural Eng. /Earthquake Eng., JSCE. 20(1) 1s-11s.

Yun, H., Kyriakides, S., 1990. On the beam and shell modes of buckling of buried pipelines. Soil Dynamics and Earthquake Engineering. 9,179-193.

Wang J.N. (1993) Seismic design of tunnels: A simple state of the art design approach. Parsons Brinckerhoff Inc., New York.

Zerva, A., 1994. On the spatial variation of seismic ground motions and its effects on lifelines. Engineering Structures. 16, 534-546.

Zerva A., 2009. Spatial variation of seismic ground motions: Modeling and engineering applications. Boca Raton, CRC Press, Taylor & Francis Group.

Zerva, A., Ang, A.-S, Wen, Y.K., 1985. A study of seismic ground motion for lifeline response analysis. Department of Civil Engineering, University Illinois Urbana-Champaign.

List of Figures

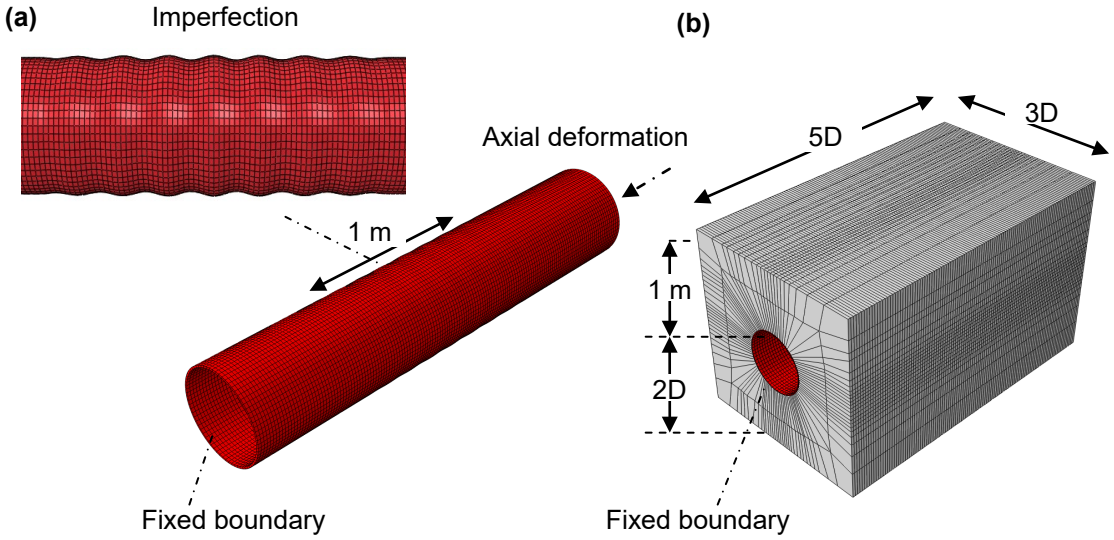

Figure 1. Representative numerical models of (a) above ground and (b) embedded pipe segments developed in ABAQUS to examine the effects of salient parameters on the axial response of NG pipelines (adapted after Tsinidis et al., 2018).

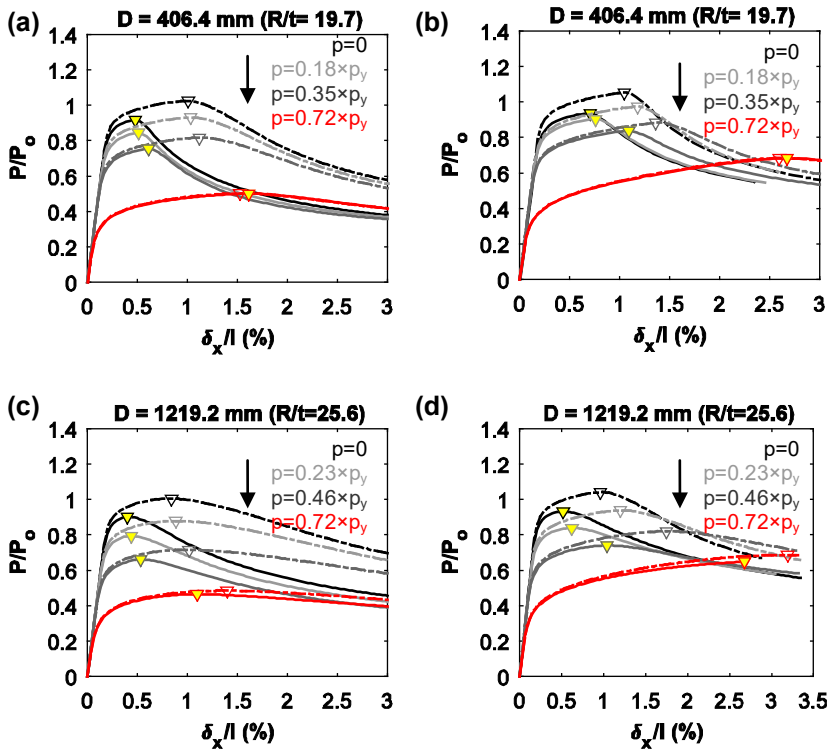

Figure 2. Average axial load- deformation paths computed for various levels of internal pressure for (a) an above ground pipe segment with R/t = 19.7, (b) a buried pipe segment with R/t = 19.7, (c) an above ground pipe segment with R/t = 25.6, (d) a buried pipe segment with R/t = 25.6 (p_y: pressure corresponding to yield stress of the pipe, dashed lines: perfect segments, solid lines: segments with initial geometric imperfection, w/t =0.1).

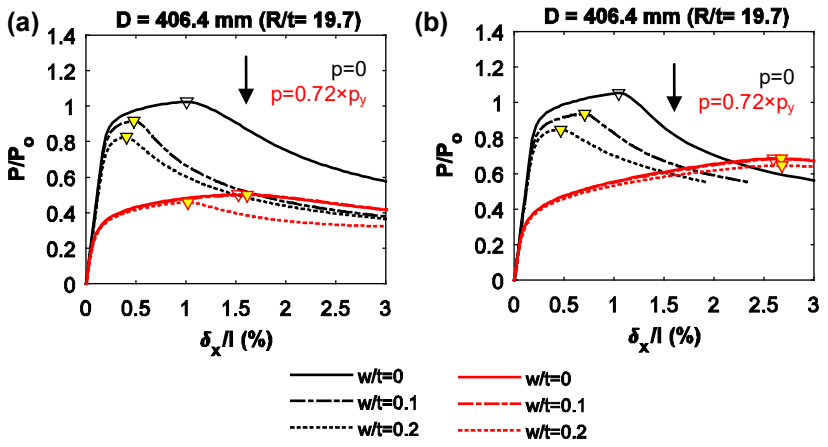

Figure 3. Average axial load-deformations paths of (a) above ground and (b) embedded pipe segments of a steel pipeline with diameter D = 406.4 mm and radius over thickness ratios R/t = 19.7, computed for various amplitudes of initial geometric imperfections of the pipe walls.

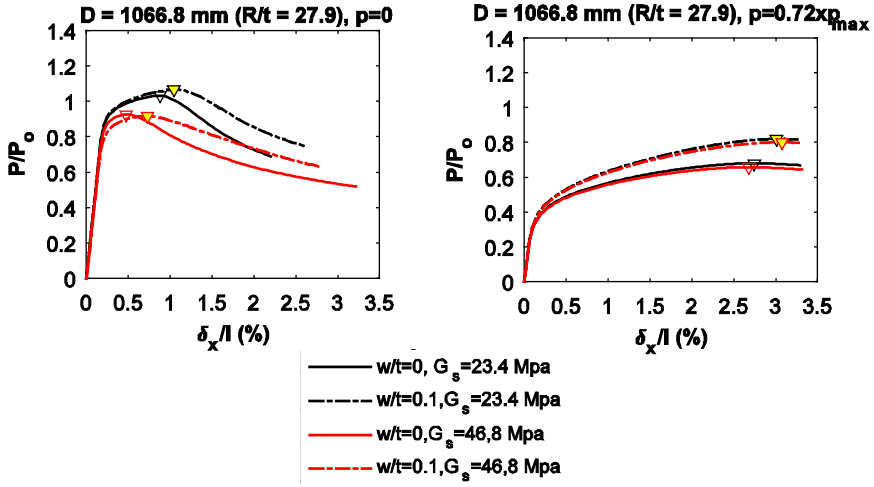

Figure 4. Effect of the stiffness of the trench soil on the average axial load-deformation paths computed for non-pressurized or pressurized segments of a pipeline with diameter D = 1066.8 mm and radius over thickness ratio R/t = 27.9) by either considering or neglecting the initial geometric imperfections.

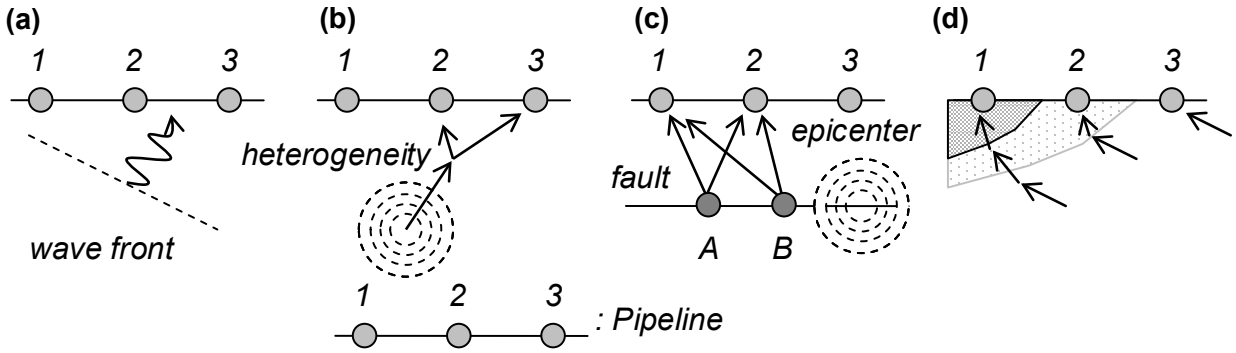

Figure 5. Sources of spatial variation of the ground seismic motion across a pipeline axis of extended length: (a) wave passage effect, (b) extended source effect, (c) ray-path effect, (d) local site effects.

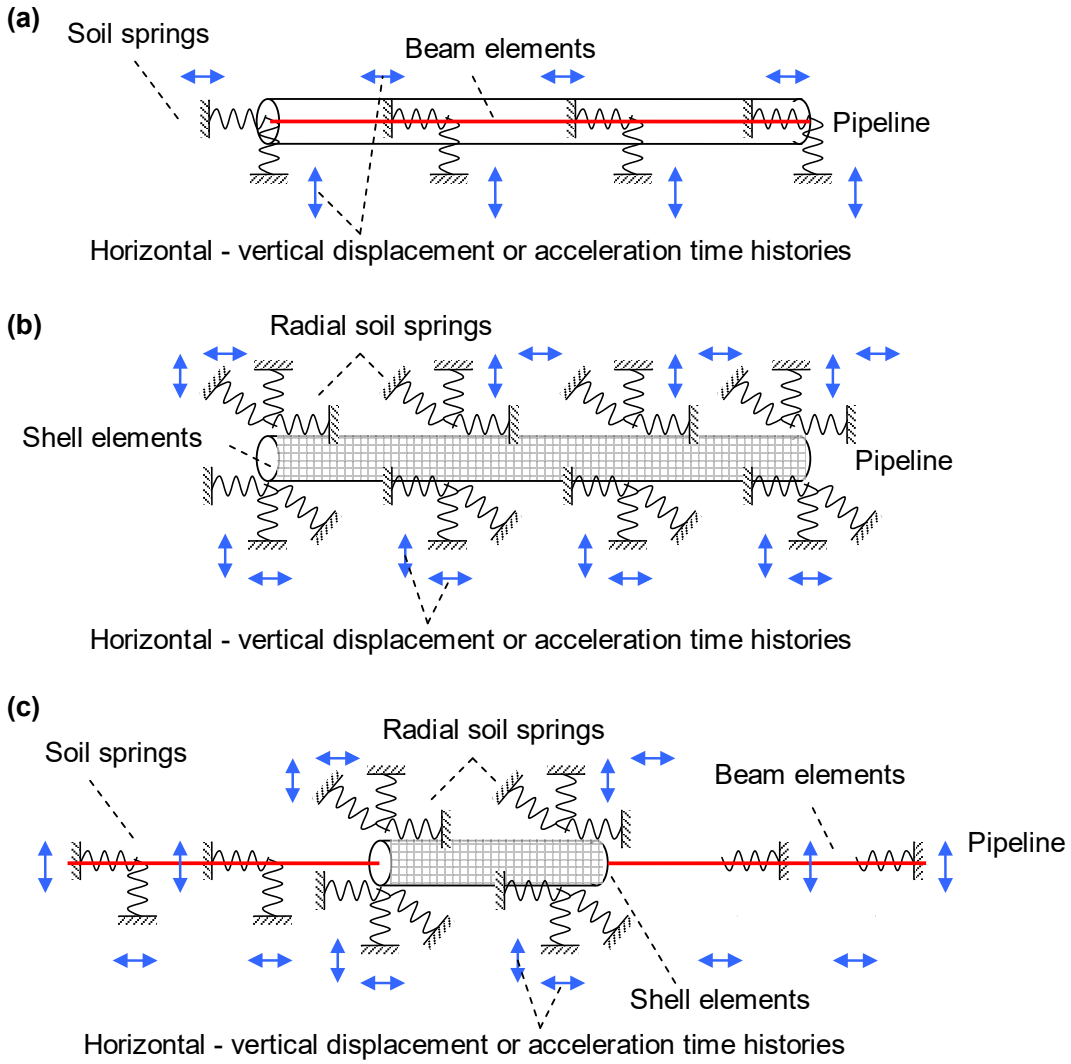

Figure 6. Alternatives of SPI models, (a) beam pipe model on soil springs, (b) shell pipe model on soil springs, (c) hybrid beam-shell pipe model on soil springs.

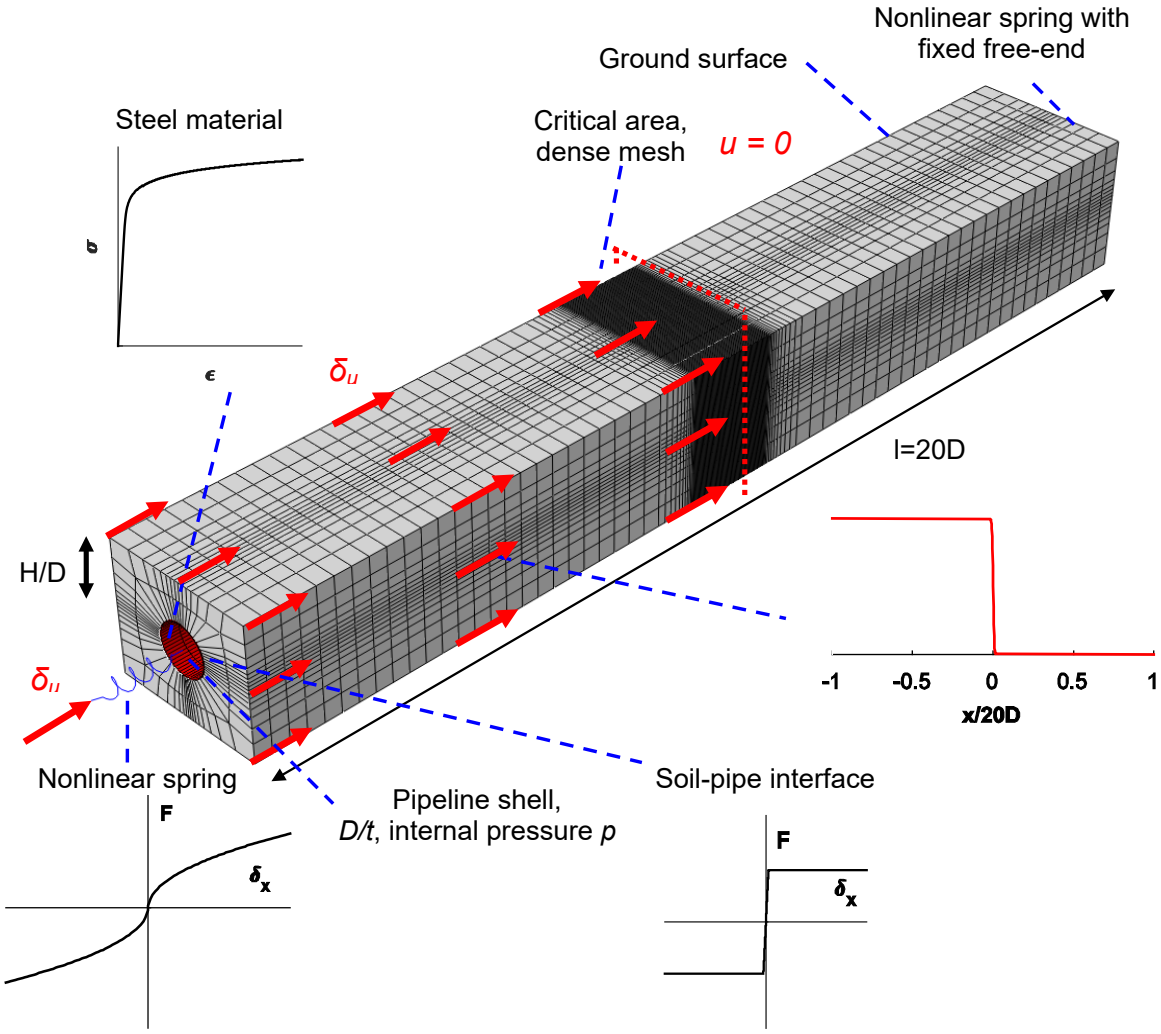

Figure 7. 3D numerical model of a buried steel NG pipeline-trench soil configuration, developed in ABAQUS (ABAQUS, 2012) to examine the seismic vulnerability of the pipeline under local buckling failures near a geotechnical discontinuity, potentially caused by differential seismically-induced axial ground deformations.

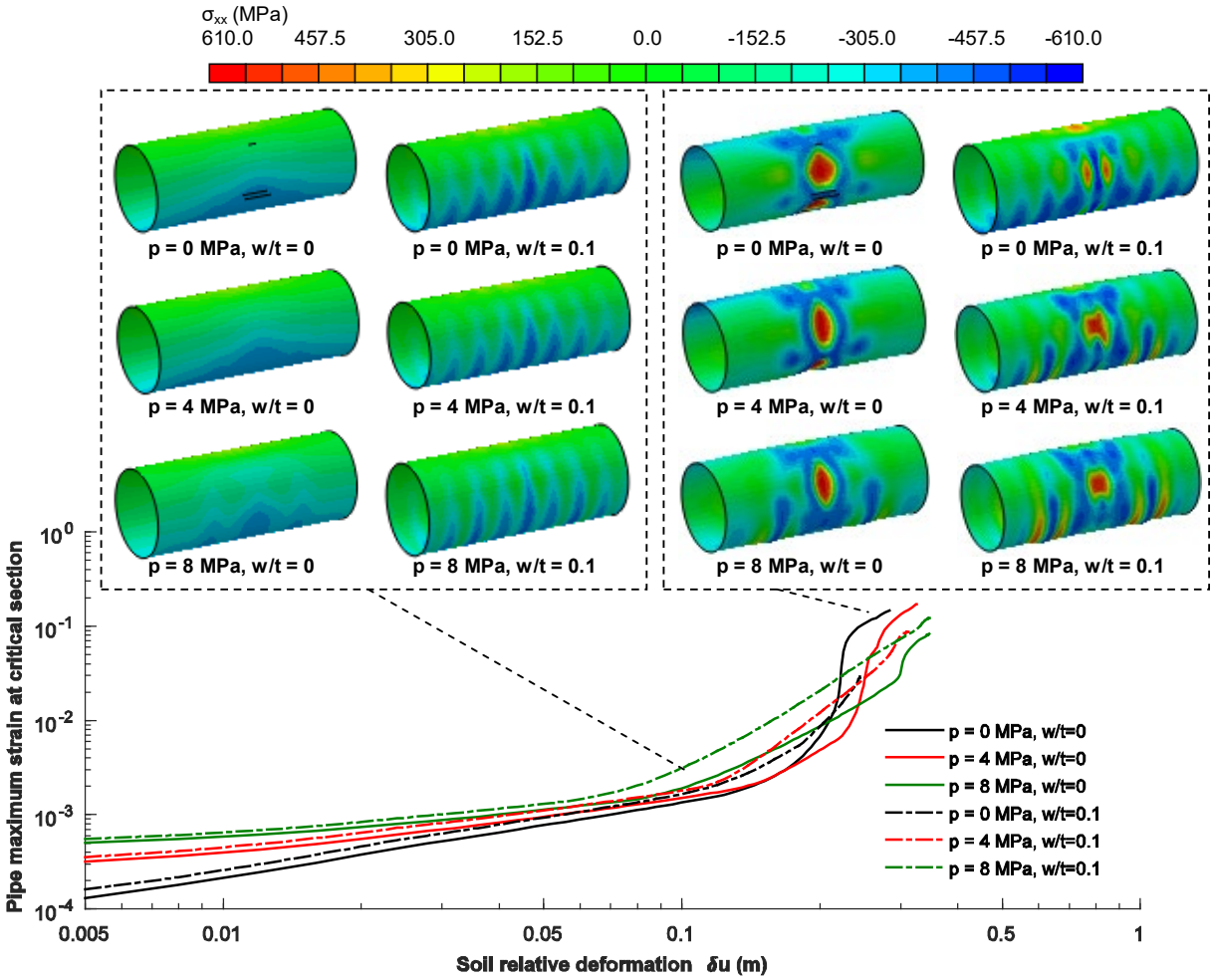

Figure 8. Effects of internal pressure and geometric imperfection of the pipe walls on the axial stresses and the evolution of the maximum compressive strain, computed at the critical pipeline section for an increasing relative axial ground deformation δ_u (results for a D = 762 mm pipeline, embedded in trench soil A).

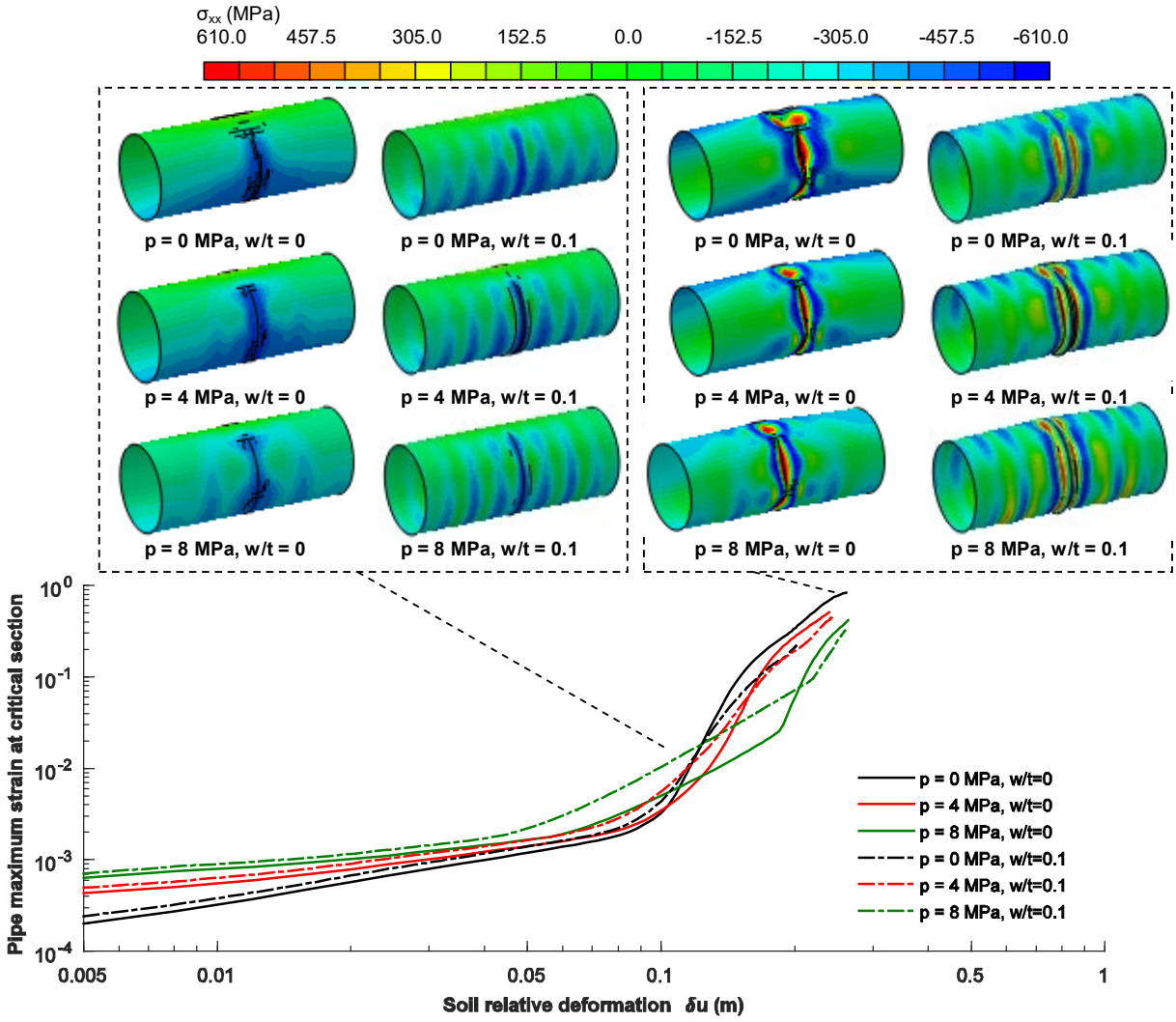

Figure 9. Effects of internal pressure and geometric imperfection of the pipe walls on the axial stresses and the evolution of the maximum compressive strain, computed at the critical pipeline section for an increasing relative axial ground deformation δ_u (results for a D = 762 mm pipeline, embedded in trench soil B).

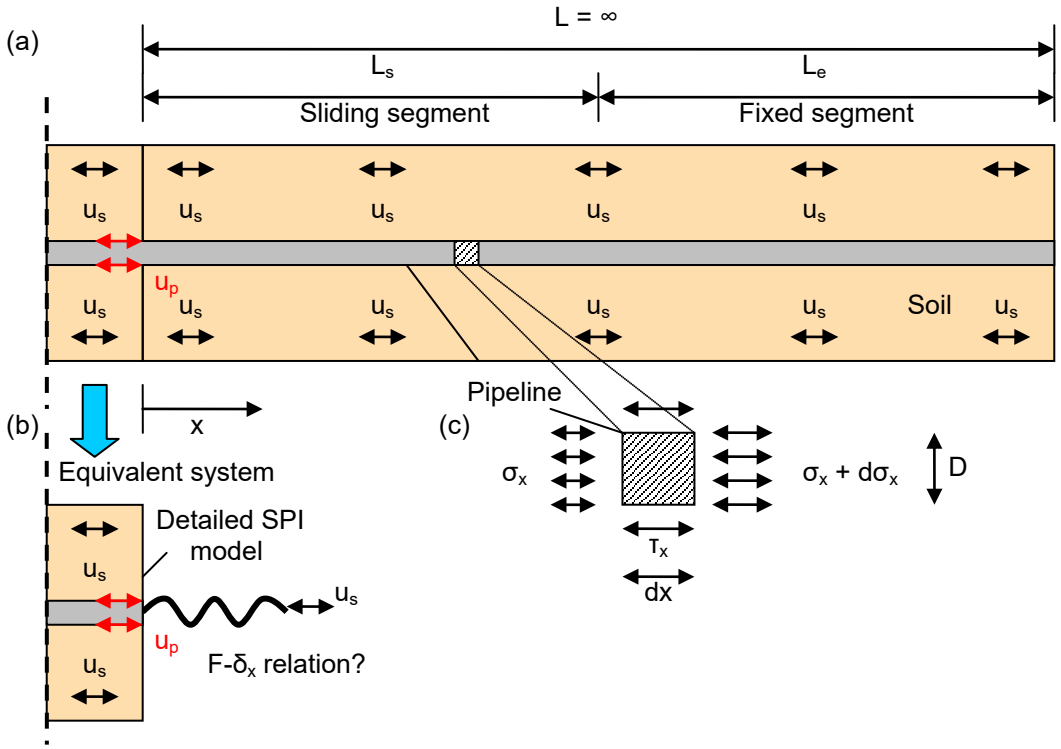

Figure A1. Buried pipeline subjected to a soil movement due to seismically-induced in plane transient ground deformations. Half view of (a) the detailed long 3D SPI model and (b) the 3D SPI hybrid model with nonlinear springs at the end boundaries. (c) Free-bode diagram of the pipeline segment.

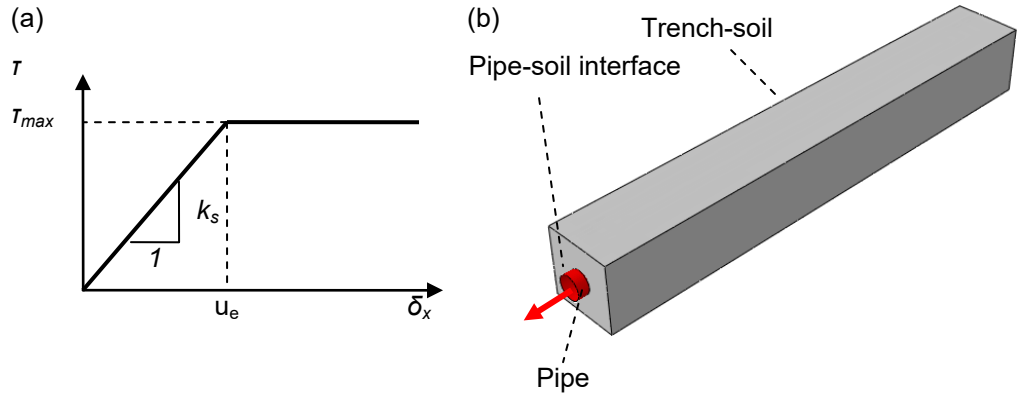

Figure A2. (a) Shear stress-displacement relationship of the soil-pipe interface. (b) Numerical pull-out simulation of pipeline from the trench soil for the evaluation of the shear strength and stiffness of the soil-pipe interface.

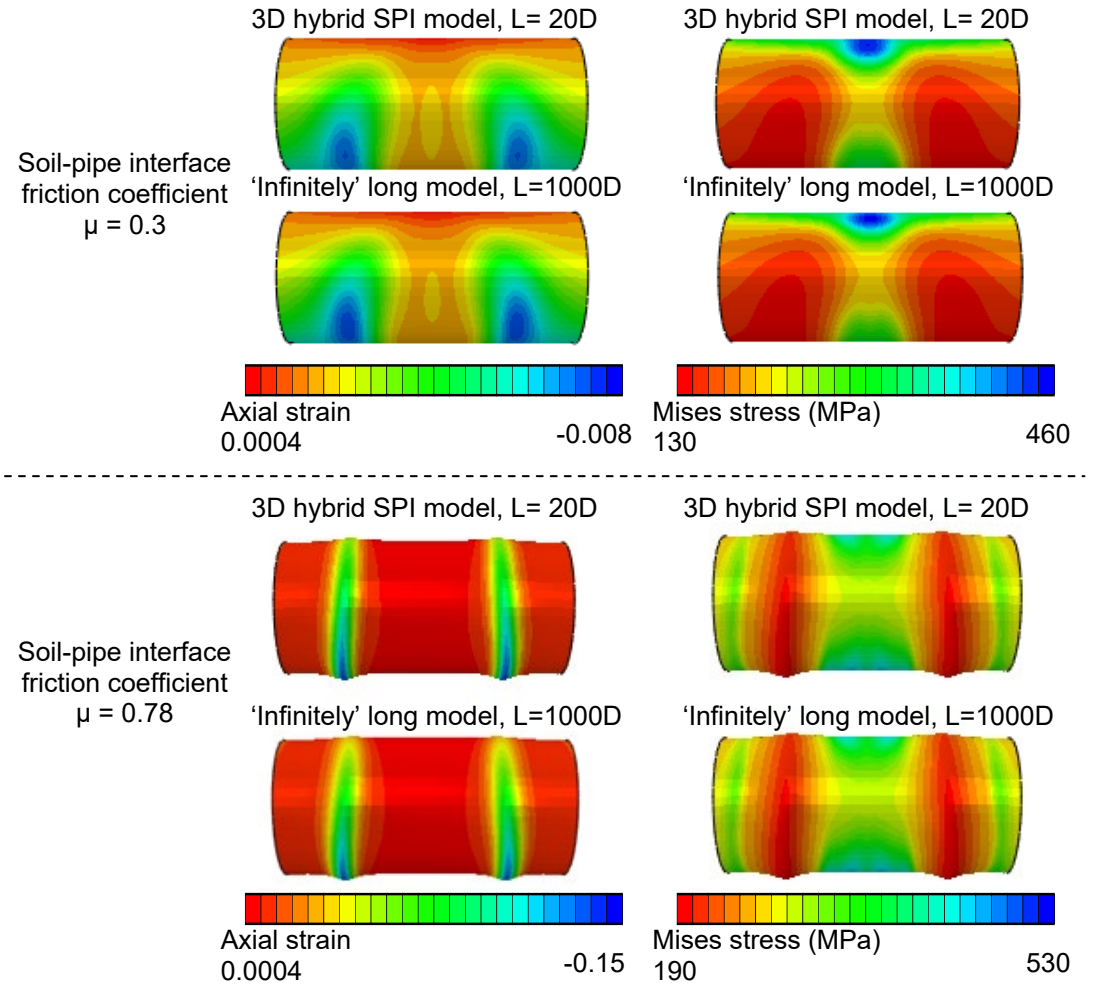

Figure A3. Contour diagrams of the Mises stresses and axial strains distributions computed at the critical central section of a D = 914.4 mm buried pipeline by the 3D hybrid SPI model and an 'infinitely' long equivalent 3D SPI model.

List of Tables

Table 1. Ultimate soil force – relative displacement relationships proposed by ALA (2001) for simulation of the soil-pipe relative motion.

Spring direction	Ultimate soil restraint force	Ultimate soil-pipe relative displacement
Axial	$\pi Dac + 0.5\mu\gamma' H\left(1+k_0\right)\pi D$	3 □ 10 *mm*
Lateral	$cDN_{ch} + \gamma' DHN_{qh}$	$0.04\left(H + D/2\right) \le 0.10D$ □ $0.15D$
Uplift, vertical	$cDN_{cv} + \gamma' DHN_{qv}$	$0.01H$ □ $0.02H \le 0.10D$ for dense to loose sands $0.1H$ □ $0.2H \le 0.20D$ for stiff to soft clays
Bearing, vertical	$cDN_c + \gamma' DHN_{qb} + 0.5\gamma D^2 N_\gamma$	$0.10D$ for granular soils $0.20D$ for cohesive soils

πD: circumference of the pipe, a :adhesion factor, c: trench soil cohesion, μ: friction coefficient of the soil-pipe interface, γ': effective unit weight of the trench soil, H: depth to the pipe centreline, k_0: coefficient of lateral earth pressure, $N_{ch}, N_{qh}, N_{cv}, N_{qv}, N_{qb}, N_{qv}, N_c, N_\gamma$: bearing capacity factors in the horizontal vertical uplift and vertical bearing direction (subscripts q, γ stand sand, c denotes clay).

Table 2. Main advantages, disadvantages and range of applicability of the methods presented herein

Method	**Advantages**	**Disadvantages**	**Range of applicability**
'Free-field' analysis methods	• Easy to apply	• SPI effects are neglected • Critical damage modes of steel pipelines can not be simulated. • Salient parameters affecting the seismic response and vulnerability of buried steel pipelines (i.e. internal pressure, geometric wall imperfections, soil-pipe interface characteristics) can not be considered	• Buried pipelines whose stiffness is significantly lower than the one of the surrounding ground • Inadequate for the design and assessment of 'stiff' pipelines, i.e. pipelines with low radius over thickness (R/t) ratios, like the steel pipelines commonly used in NG applications
Beam or shell element pipe models on soil springs	• Easy to apply • Computationally efficient method	• Available soil springs refer to uniform soil deposits • Coarse meshes may lead to inaccurate predictions of the pipeline stresses and strains, particularly in case of pipelines with geometric wall imperfections • The simulation of soil compliance by means of simple elasto-plastic soil springs might be debatable in case of significant soil nonlinearities during ground shaking	• Buried pipelines in relatively uniform soil deposits, which are exhibiting reduced nonlinear response during ground shaking

3D continuum models of the pipe-trench soil system	• The method allows for a more accurate simulation of geometric imperfections of the pipeline walls • The method allows for the use of sophisticated contact models which may replicate more accurately the potential geometrical nonlinear phenomena along the soil-pipe interface during ground shaking • The method may account for critical parameters affecting the buckling response of steel pipelines, e.g. internal pressure, geometric wall imperfections etc	• The method is computationally more demanding and time consuming, since a sufficient length of the soil-pipe system is required to account for the effect of the length of the configuration on its axial response	• Buried pipelines crossing critical areas, e.g. predefined geotechnical discontinuities, valley boundaries etc.
3D hybrid continuum models of the pipe-trench soil system	• A The method allows for a more accurate simulation of geometric imperfections of the pipeline walls • The method allows for the use of sophisticated contact models which may replicate more accurately the potential geometrical nonlinear phenomena along the soil-pipe interface during ground shaking • Computational efficiency compared to the 'infinitely' long 3D continuum models of the pipe-trench soil system • The method may account for critical parameters affecting the buckling response of steel pipelines, e.g. internal pressure, geometric wall imperfections etc	• The method is computationally more demanding and time consuming, compared to the beam or shell element pipe models on soil springs	• Buried pipelines crossing critical areas, e.g. predefined geotechnical discontinuities, valleys etc.

1
2